

# Scalable and non-iterative graphical model estimation

Kshitij Khare, *Dept. of Statistics, University of Florida*

Syed Rahman, *Apple Inc.*

Bala Rajaratnam, *Dept. of Statistics, UC Davis*

Jiayuan Zhou, *Freddie Mac*

## Abstract

Graphical models have found widespread applications in many areas of modern statistics and machine learning. Iterative Proportional Fitting (IPF) and its variants have become the default method for undirected graphical model estimation, and are thus ubiquitous in the field. As the IPF is an iterative approach, it is not always readily scalable to modern high-dimensional data regimes. In this paper we propose a novel and fast non-iterative method for positive definite graphical model estimation in high dimensions, one that directly addresses the shortcomings of IPF and its variants. In addition, the proposed method has a number of other attractive properties. First, we show formally that as the dimension  $p$  grows, the proportion of graphs for which the proposed method will outperform the state-of-the-art in terms of computational complexity and performance tends to 1, affirming its efficacy in modern settings. Second, the proposed approach can be readily combined with scalable non-iterative thresholding-based methods for high-dimensional sparsity selection. Third, the proposed method has high-dimensional statistical guarantees. Moreover, our numerical experiments also show that the proposed method achieves scalability without compromising on statistical precision. Fourth, unlike the IPF, which depends on the Gaussian likelihood, the proposed method is much more robust.

*Keywords:* Graphical models, ultra high-dimensions, non-iterative estimation, Cholesky decomposition

## 1 Introduction

Sparse covariance estimation and graphical models have become a staple of modern statistical inference and machine learning. They have also found widespread use in a spectrum of application areas. In this paper we specifically focus on the large class of undirected (or concentration) graph models, where some entries of the inverse covariance matrix  $\Omega$  are restricted to be zero. These models have been of significant interest in recent years, especially as high-dimensional datasets with tens of thousands of variables or more have become increasingly common. The cases when the underlying distribution is Gaussian has also been of

special interest. Under this assumption, zeroes in the concentration matrix imply conditional independencies.

Suppose  $\mathbf{Y}_1, \mathbf{Y}_2, \dots, \mathbf{Y}_n$  are i.i.d. observations from a distribution on  $\mathbb{R}^p$ . Let  $\Sigma$  denote the covariance matrix, and let  $\Omega = \Sigma^{-1}$  denote the concentration matrix or the inverse covariance matrix of this distribution. There are often two tasks involved in the statistical analysis of undirected graphical models. The first is *model or graph selection*, or identifying the pattern of structural zeros in  $\Omega$ . The second is *positive definite estimation*, i.e., finding a positive definite (p.d.) estimate of  $\Sigma$  under the discovered sparsity pattern. Such positive definite estimates are often required for downstream applications where the covariance estimate is a critical ingredient in multivariate analysis techniques. Examples of such applications are widespread in the biomedical, environmental and social sciences.

A number of useful methods have been proposed for positive definite inverse covariance matrix estimation consistent with a given sparsity pattern. For Gaussian undirected graphical models, the MLE cannot be obtained in closed form unless the pattern of zero restrictions corresponds to a decomposable or chordal graph (see Lauritzen [1996]). A novel iterative algorithm called iterative proportional fitting (IPF) was proposed by Speed and Kiveri [1986] to obtain the MLE in this case. Over the last few decades, the IPF estimation method has become synonymous with undirected graphical model estimation for a given sparsity pattern. Several faster modifications and adaptations of IPF have been proposed in recent years, highlighting the contemporaneous nature of this line of research, see for example Hara and Takemura [2010], Xu et al. [2011, 2012, 2015], Hojsgaard and Lauritzen [2023]. These iterative algorithms rely on sequential updates to relevant sub-matrices of  $\Sigma$  or  $\Omega$  based on the given sparsity pattern.

A different approach which obtains the MLE by modifying the Glasso algorithm to take the known sparsity pattern into account has been developed in [Hastie et al., 2009, Algorithm 17.1]. The likelihood is maximized one row at a time using block coordinate-wise ascent. We refer to this algorithm as the G-IPF algorithm. There is also substantial literature on Bayesian estimation for Gaussian undirected graphical models, see Dawid and Lauritzen [1993], Roverato [2002], Letac and Massam [2007], Rajaratnam et al. [2008], Mitsakakis et al. [2011], Lenkoski [2013] and the references therein. Numerical approaches for estimation in undirected graphical models such as the IPF and its variants, and the G-IPF, all tend to employ computationally intensive iterative algorithms which have to be repeated until convergence. The iterative nature of these algorithms thus does not always render them immediately scalable to the modern setting where scalability is a real necessity. Such modern regimes pose a significant challenge in the sense that they require scalability without compromising on statistical precision.

As mentioned above, the iterative nature of current methods is an immediate impediment to scalability, in the sense that numerical computations of a high order have to be repeated, thus resulting in a prohibitive computational burden. Hence, it is critical to construct a possibly *non-iterative method* which is able to provide a *positive definite estimate of  $\Omega$  which is consistent with a given general sparsity pattern*. A new estimation framework, one which is specifically designed for and addresses the high dimensional nature of the problem, is required. We address this crucial gap in the literature by introducing a non-iterative method, called CCA, for positive definite estimation in undirected graphical models with an **arbitrary** sparsity pattern in the concentration matrix. The method is comprised of two steps and can be summarized as follows: In the first step, estimates are obtained for a pattern of

zeros corresponding to an appropriate larger chordal graph. As the approximating graph is chordal, estimates can be immediately computed in closed form, circumventing repeated iterations. In the second step, the Cholesky decompositions of such estimates are then suitably modified to obtain estimates with the original pattern of zeroes in the concentration matrix. These steps together yield an approach which obviates the need to employ computationally expensive iterative algorithms when dealing with non-chordal concentration graphical models. Specifically, the chordal graph serves as an important conduit to obtaining the desired concentration graph estimates. Notably, methods such as the IPF and its modern variants require repetition of its iterations until convergence, while no such repetition is necessary for the CCA algorithm. Thus, the proposed CCA algorithm provides significant computational savings compared to IPF or G-IPF. Moreover, in several settings the computational complexity of the CCA algorithm is smaller than even a single iteration of the G-IPF algorithm (see Section 3.2 for examples), bearing in mind that the G-IPF iterations have to be repeated thereafter till convergence. We demonstrate both theoretically and numerically that substantial computational improvements can be obtained using the proposed approach, while maintaining similar levels of statistical precision as state-of the art approaches.

In addition to the introduction of a novel non-iterative estimation framework, the proposed CCA approach has multiple other benefits - from both a theoretical and methodological perspective. Recall that the IPF and its variants fundamentally depend on the functional form of the Gaussian likelihood. On the contrary, the proposed CCA approach can instead also be formulated in a non-parametric way yielding a more robust estimator, thus making it more immune to the effect of outliers. CCA also enjoys high dimensional statistical guarantees. The proposed CCA approach has yet another significant benefit in the sense it can be readily coupled with any scalable thresholding method for obtaining a sparsity pattern/ pattern of zeros in the inverse covariance matrix. More specifically, non-iterative thresholding based methods for model selection, such as the HUB screening method in Hero and Rajaratnam [2012], and the recently proposed FST method in Zhang et al. [2021], are equipped with high-dimensional statistical guarantees and are generally much faster and scalable to significantly higher dimensional settings than the penalized likelihood methods which use iterative optimization algorithms. To clarify, the term non-iterative sparsity selection method refers to a method which requires a fixed and finite amount of time, and does not need repetitions until convergence. However, such thresholding based methods, though very useful, are not guaranteed to produce positive definite estimates of  $\Omega$ , which in turn could hinder their use in downstream applications which require a positive definite estimate of the covariance matrix (see for example Ledoit and Wolf [2003], Guillot et al. [2015]). Coupling the proposed CCA approach with scalable thresholding methods however guarantees computational efficiency and scalability of the whole procedure as well as positive definiteness of the final inverse covariance matrix estimate. In principle, the proposed CCA approach can also be combined with  $\ell_1$ -penalized methods: Recall that  $\ell_1$ -penalized methods such as CONCORD (Khare et al. [2015]) yield sparse inverse covariance matrix estimates but are not guaranteed to yield positive definite estimates. Here, one can employ the proposed CCA approach to produce a p.d. estimator which is consistent with a sparsity pattern induced by any  $\ell_1$ -penalized method.

The paper is organized as follows. Section 2 provides required preliminaries. The proposed positive definite estimation method is introduced in Section 3. A thorough evaluation of its computational complexity is provided in Section 3.2. In Section 4 we establish asymp-

totic consistency of the proposed estimates in the high-dimensional setting where the number of variables increases with sample size. Detailed experimental evaluation, validation and applications to real data is undertaken in Section 5.

## 2 Preliminaries

In this section we provide the required background material from graph theory and matrix algebra.

### 2.1 Graphs and vertex orderings

A graph  $G = (V, E)$  consists of a finite set of vertices  $V$  (not necessarily ordered) with  $|V| =: p$ , and a set of edges  $E \subseteq V \times V$ . We consider undirected graphs with no loops. Hence,  $(v, v) \notin E$  for every  $v \in V$ , and  $(u, v) \in E \Rightarrow (v, u) \in E$ . Next, we define the notions of vertex ordering and ordered graphs. These are necessary in subsequent analysis.

**Definition 1** (*Vertex ordering*) *A vertex ordering  $\sigma$  of the vertex set  $V$  is a bijection from  $V$  to  $V_p := \{1, 2, \dots, p\}$ .*

**Definition 2** (*Ordered graph*) *Consider the undirected graph  $G = (V, E)$  and an ordering  $\sigma$  of  $V$ . The ordered graph  $G_\sigma$  has vertex set  $V_p$  and edge set  $E_\sigma = \{(\sigma(u), \sigma(v)) : (u, v) \in E\}$ .*

### 2.2 Cholesky decomposition

Given a positive definite matrix  $\Omega \in \mathbb{P}_p^+$ , there exists a unique lower triangular matrix  $L$  with positive diagonal entries such that  $\Omega = LL^T$ , where  $L$  is the “Cholesky factor” of  $\Omega$ . The Cholesky decomposition will be a useful ingredient in the estimators constructed in this paper.

### 2.3 The spaces $\mathbb{P}_{G_\sigma}$ and $\mathbb{L}_{G_\sigma}$

Let  $G = (V, E)$  be a graph on  $p$  vertices and let  $\sigma$  be an ordering of  $V$ . Let  $\mathbb{P}^+$  denote the space of  $p \times p$  positive definite matrices, and  $\mathbb{L}^+$  denote the space of  $p \times p$  lower triangular matrices with positive diagonal entries. We consider two matrix spaces that will play an important role in our analysis. The first matrix space

$$\mathbb{P}_{G_\sigma} = \{\Omega \in \mathbb{P}^+ : \Omega_{ij} = 0 \text{ if } i \neq j \text{ and } (i, j) \notin E_\sigma\},$$

is the collection of all  $p \times p$  positive definite matrices where the  $(i, j)^{th}$  entry is zero if  $i$  and  $j$  do not share an edge in the ordered graph  $G_\sigma$ . The other matrix space

$$\mathbb{L}_{G_\sigma} = \{L \in \mathbb{L}^+ : LL^T \in \mathbb{P}_{G_\sigma}\},$$

is the collection of all  $p \times p$  lower triangular matrices with positive diagonal entries, which can be obtained as a Cholesky factor of a matrix in  $\mathbb{P}_{G_\sigma}$ .

## 2.4 Decomposable graphs

An undirected graph  $G$  is said to be *decomposable* if it is connected and does not contain a cycle of length greater than or equal to four as an induced subgraph. The reader is referred to Lauritzen [1996] for all the common notions of graphical models (and in particular decomposable graphs) that we will use here. One such important notion is that of a perfect vertex elimination scheme.

**Definition 3** *An ordering  $\sigma$  of  $V$  is defined to be a perfect vertex elimination scheme for a decomposable graph  $G$  if for every  $u, v, w \in V$  such that  $\sigma(u) > \sigma(v) > \sigma(w)$  and  $(\sigma(u), \sigma(w)) \in E_\sigma, (\sigma(v), \sigma(w)) \in E_\sigma$ , then  $(\sigma(u), \sigma(v)) \in E_\sigma$ .*

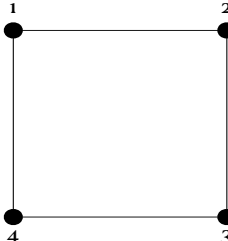
## 2.5 Cholesky factors and fill-in entries

Let  $G$  be a decomposable graph, and  $\sigma$  an ordering of  $V$ . Paulsen et al. [1989] prove that  $\sigma$  is a perfect vertex elimination scheme for  $G$  if and only if

$$\mathbb{L}_{G_\sigma} = \{L \in \mathbb{L}^+ : L_{ij} = 0 \text{ if } i > j, (i, j) \notin E_\sigma\},$$

i.e, the structural zeroes in every matrix in  $\mathbb{P}_{G_\sigma}$  are also reflected in its Cholesky factor.

However, if the graph  $G$  is non-decomposable, or if  $G$  is decomposable but  $\sigma$  is not a perfect vertex elimination scheme, then for any matrix in  $\mathbb{P}_{G_\sigma}$ , the zeroes in the Cholesky factor are in general a subset of the structural zeroes in  $\mathbb{P}_{G_\sigma}$ . The extra non-zero entries in the Cholesky factor are referred to as the *fill-in* entries corresponding to  $\mathbb{P}_{G_\sigma}$ . For example, consider the non-decomposable 4-cycle graph  $G = (V, E)$  below where  $\sigma$  is such that  $E_\sigma = \{(1, 2), (2, 3), (3, 4), (4, 1)\}$  with  $\Omega$  and  $L$  specified as below.



$$, \Omega = \begin{pmatrix} 3 & 1 & 0 & 1 \\ 1 & 3 & 1 & 0 \\ 0 & 1 & 3 & 2 \\ 1 & 0 & 2 & 3 \end{pmatrix} \quad \text{and} \quad L = \begin{pmatrix} 1.732 & 0 & 0 & 0 \\ 0.577 & 1.633 & 0 & 0 \\ 0 & 0.612 & 1.620 & 0 \\ 0.577 & -0.204 & 1.312 & 0.951 \end{pmatrix}.$$
(1)

Note that  $\Omega \in \mathbb{P}_{G_\sigma}$ , and it can be shown that  $L$  above is its Cholesky factor. Clearly, the zero entries in the lower triangle of  $L$  are a strict subset of the zero entries in  $\Omega$ . The fill-in entry in this case is the  $(4, 2)^{th}$  entry. Next, we define the notion of a filled graph.

**Definition 4** *Given an ordered graph  $G_\sigma$ , the filled graph for  $G_\sigma$ , denoted by  $G_\sigma^D = (V_p, E_\sigma^D)$ , is defined as follows:*

1.  $G_\sigma^D$  is an ordered decomposable graph, i.e.,  $G_D$  is a decomposable graph and  $\sigma$  is a perfect vertex elimination scheme for  $G_D$ .
2. For every  $\Omega \in \mathbb{P}_{G_\sigma}$ , the corresponding Cholesky factor  $L$  satisfies  $L_{ij} = 0$  if  $i > j, (i, j) \notin E_\sigma^D$ .
3. The edge set  $E_\sigma^D$  of  $G_\sigma^D$  is a subset of the edge set of every graph satisfying properties 1 and 2.

Essentially, the filled graph for  $G_\sigma$  is the “minimal” (ordered) decomposable graph whose edge set contains  $E_\sigma$  along with all the edges corresponding to the fill-in entries for matrices in  $L_{G_\sigma}$ , i.e., a “decomposable cover” for  $G_\sigma$ . In the 4-cycle example considered above, the filled graph  $G_\sigma^D$  has edge set given by

$$E_\sigma^D = \{(1, 2), (2, 3), (3, 4), (4, 1), (4, 2)\}.$$

For given  $G$  and  $\sigma$ , a simple procedure to obtain  $G_\sigma^D$  called the elimination tree method (see Davis [2006]) is given below.

1. Start with  $E_\sigma^D = E_\sigma$ . Set  $k = 1$ .
2. Let  $\mathcal{N}_k^> = \{j : j > k, (j, k) \in E_\sigma^D\}$ . Add necessary edges to  $E_\sigma^D$  so that  $\mathcal{N}_k^>$  is a clique.
3. Set  $k = k + 1$ . If  $k < p - 1$ , go to Step 1.

## 2.6 Choice of the ordering $\sigma$

The proposed CCA method presented in the next section will require Cholesky decompositions of appropriate positive definite matrices. Since the Cholesky decomposition inherently uses an ordering of the variables, the choice of this ordering is an important issue which needs to be addressed in a principled way. In several applications, a natural domain-specific ordering of the variables based on time, location etc. is available (see examples in Huang et al. [2006], Rajaratnam et al. [2008], Shojaie and Michailidis [2010], Yu and Bien [2017], Khare et al. [2019]). However, in other applications a natural ordering is not always available. In such settings, we can choose the ordering of the variables based on computational considerations as follows. Note that the decomposable cover  $G_\sigma^D$  is a function of the ordering  $\sigma$ . As we shall see in Section 3, it is important to choose  $\sigma$  which gives as fewer fill-in entries as possible, i.e., the number of extra edges in  $E_\sigma^D$  as compared to  $E_\sigma$ . This problem is well-studied in the computer science literature. In fact, it is an NP-hard problem which makes it challenging to solve in practice (see Davis [2006] and the references therein). However, several heuristic methods have been developed to solve this problem, including the Reverse Cuthill-McKee (RCM) method, which is implemented in the *chol* function in R. We refer to the ordering produced by this method as the *RCM fill reducing ordering*. In subsequent analysis, we choose  $\sigma$  as the RCM ordering in case a natural ordering of the variables is not available.

# 3 A non-iterative Gaussian graphical model estimator

## 3.1 Methodology: The constrained Cholesky approach

Suppose  $\mathbf{Y}_1, \mathbf{Y}_2, \dots, \mathbf{Y}_n$  are i.i.d. observations from a distribution on  $\mathbb{R}^p$  with covariance matrix  $\Sigma$  and concentration matrix  $\Omega = \Sigma^{-1}$ . The sparsity pattern in  $\Omega$  is assumed to be given, as encoded by the graph  $G$ . When the distribution is multivariate Gaussian, the zeros in  $\Omega$  signify conditional independence between the relevant variables, and  $G$  can be interpreted as a *conditional independence graph*. Even when the underlying distribution is not Gaussian, sparsity in  $\Omega$  signifies the lack of relevant partial correlations, and  $G$  can be interpreted as a *partial correlation graph*. In several applications,  $G$  is not available based on

domain-specific knowledge, in which case we use an estimate of  $G$  provided by a thresholding based approach such as *FST* (Zhang et al. [2021]). As specified earlier, similar to the IPF our goal is to find a p.d. estimate of  $\Omega$  consistent with a given sparsity pattern, but one that is scalable to modern data regimes. For a given  $\sigma$  (or one obtained by RCM fill reducing approach), the task considered in this sub-section is to find a positive-definite estimate of  $\Omega$  lying in  $\mathbb{P}_{G_\sigma}$ , without recourse to iterative approaches.

Before we formally describe the specific aspects of the CCA methodology, we first provide an intuitive description of the two steps which encapsulate the proposed CCA method. Recall that graphical model estimation for a general non-decomposable graph faces three significant challenges (especially in high-dimensional settings): (1) lack of a closed form solution warranting an iterative procedure (such as the IPF), (2) the graphical model constraint where estimates need to lie in the correct parameter space (i.e., the prescribed zero pattern), and (3) the more nuanced and “delicate” positivity requirement (note that the sparsity and positivity constraints constitute two distinct hurdles).

CCA specifically recognizes the above three challenges and provides a solution which overcomes all three of them in a computationally tractable manner. The order in which this is undertaken is crucial. First, CCA circumvents the need for an iterative procedure by transferring the problem from the given graph  $G$  to a decomposable cover of  $G$  (as denoted by  $G^D$ ). Doing so, ensures that a closed form solution is obtained for a problem which is “close” to the original estimation problem. Transferring the problem to a decomposable cover, however, introduces additional edges in the graph  $G^D$  which are not present in the original graph  $G$ , i.e., some of the required zeros in the precision matrix estimator are lost (the additional parameters in  $\hat{\Omega}^D$  are referred to as “fill-in entries”, the reason for which will become clear very soon). More specifically, the issue with the resulting decomposable graph estimator is that it does NOT have the correct sparsity pattern - though it is positive definite. As positivity is a more “delicate” property, it can be easily lost if one zeros out the resulting decomposable estimator to achieve the desired sparsity pattern. In anticipation of the risk of losing positivity while aiming for the correct sparsity pattern, the resulting decomposable graph estimator is first expressed in terms of its Cholesky decomposition (which is available in closed form thus avoiding any iterative procedure). There are two reasons for this. The first reason is that if the correct vertex ordering is used, the zeros in  $\hat{\Omega}^D$  are preserved. The second reason is that the Cholesky entries do not have to obey any positivity constraints and are therefore much easier to work with. It is thus an ideal setting to work in to try and obtain the desired sparsity pattern since deforming a Cholesky does not affect positivity (provided the diagonals are positive). In summary, obtaining the decomposable cover estimator and its corresponding Cholesky transform constitute Step 1 of the CCA approach.

Armed with the closed form Cholesky estimator for the decomposable graph, the remaining task is to obtain the correct sparsity pattern for the final estimate of  $\Omega$ , i.e., to ensure that the final estimate lies in  $\mathbb{P}_{G_\sigma}$ . Here, the CCA recognizes that Cholesky entries which correspond to non-zero entries in  $\Omega$  can be regarded as functionally independent parameters in the Cholesky, whereas zeros in  $\Omega$  which are not zeros in the Choleksy are actually functionally dependent parameters (even if they appear as non-zeros in the corresponding Cholesky). This insight follows from realizing that  $\Omega$  and its Cholesky are simply two representations of the same quantity - hence the number of true functionally independent parameters in the Cholesky has to be the same as that of the  $\Omega$  (i.e., the dimension of the parameter set cannot change because of a transformation). Thus, the entries in the Choleksy which correspond

to zero entries in  $\Omega$  can be regarded as functionally dependent. With this insight in hand, CCA modifies the entries of the Cholesky corresponding to these functional independent parameters (i.e., “fill-in” entries), to obtain zeros in the corresponding positions at the level of  $\Omega$ . This process is essentially a projection of the Cholesky to the correct parameter space. Doing so enforces the desired sparsity pattern at the level of  $\Omega$ . This process of modification or adjustment of the Cholesky is facilitated by the fact that  $\Omega$  is simply its Cholesky factor multiplied by the transpose of the Cholesky factor. In other words, the quadratic relationship between  $\Omega$  and its Cholesky factor renders the adjustment of the fill-in entries a straightforward task (and importantly in closed form). In summary, note that the original graph  $G$  has a given zero pattern - some of which are lost by transferring the problem to the graph  $G^D$ . The additional edges introduced by going to  $G^D$ , and the sparsity that is lost because of this, is regained through adjusting the Cholesky parameter of  $\hat{\Omega}^D$ . The adjustment of the Cholesky to achieve the desired sparsity pattern at the level of  $\Omega$  constitutes Step 2 of the CCA approach.

Altogether, the above closed form estimation and adjustment operations completely circumvent recourse to any iterative procedure. Specifics of the CCA methodology are now described through the aforementioned two step process.

**Step I:** The first step in our approach is to find an estimator of  $\Omega$  in  $\mathbb{P}_{G_\sigma^D}$ . Recall that  $G_\sigma^D$ , which denotes the filled graph for  $G_\sigma$ , is a decomposable graph whose edge set subsumes the edge set of  $G_\sigma$ . When  $\Omega \in \mathbb{P}_{G_\sigma^D}$  and if the underlying distribution is Gaussian, the MLE  $\hat{\Omega}^D$  for  $\Omega$  is well-defined as long as  $n$  is equal to or larger than the maximal clique size in  $G_\sigma^D$ , and can be obtained in closed form (see Lauritzen [1996]). Let  $\hat{L}^D$  denote the Cholesky factor of  $\hat{\Omega}^D$ . It can be shown (see for example Atay-Kayis and Massam [2005], Roverato [2002]) that the non-zero entries of the  $j^{th}$  column of  $\hat{L}^D$  can be obtained as

$$\hat{L}_{\cdot j}^{D,>} = -\frac{(S^{>j})^{-1} S_{\cdot j}^{>}}{\sqrt{S_{jj} - (S_{\cdot j}^{>})^T (S^{>j})^{-1} S_{\cdot j}^{>}}} \text{ and } \hat{L}_{jj} = \frac{1}{\sqrt{S_{jj} - (S_{\cdot j}^{>})^T (S^{>j})^{-1} S_{\cdot j}^{>}}} \quad (2)$$

for every  $1 \leq j \leq p$ . Here for any matrix  $A$ ,  $A^{>j} := ((A_{kl}))_{k,l>j, (k,j),(l,j) \in E_\sigma^D}$  and  $A_{\cdot j}^{>} := (A_{kj})_{k>j, (k,j) \in E_\sigma^D}$ . Note that  $\hat{\Omega}^D$  lies in  $\mathbb{P}_{G_\sigma^D}$  and generally will not lie in the desired space  $\mathbb{P}_{G_\sigma}$ . We will refer to  $\hat{\Omega}^D$  and its Cholesky factor  $\hat{L}^D$  as *intermediate* estimators. Note that Step I produces estimators for  $\Omega$ -entries corresponding not only to edges in  $E_\sigma$  but also for additional edges in  $E_\sigma^D \setminus E_\sigma$ .

**Step II:** The second step in our approach is to modify or adjust the Cholesky factor  $\hat{L}^D$  to a lower triangular matrix  $\hat{L}$  such that  $\hat{\Omega} = \hat{L}\hat{L}^T \in \mathbb{P}_{G_\sigma}$ , i.e., to eliminate the additional non-zero entries in our estimate of  $\Omega$  that arise from working with a decomposable cover so that our estimator lives in the desired space. In particular, we construct  $\hat{L}$  by sequentially changing each fill-in entry of  $\hat{L}^D$  such that the corresponding entry of the concentration matrix (obtained by multiplying the resulting lower triangular matrix with its transpose) is zero. We start with the second row and move from entries with the lowest index to the highest index just before the diagonal. Whenever we encounter a fill-in entry along the way, say  $(i, j)$ , we set  $\hat{L}_{ij}$  as follows:

$$\hat{L}_{ij} = -\frac{\sum_{k=1}^{j-1} \hat{L}_{ik} \hat{L}_{jk}}{\hat{L}_{jj}}, \quad (3)$$

thereby ensuring that the  $(i, j)^{th}$  entry of the corresponding concentration matrix is zero. Note that the update in (3) only uses entries from the  $i^{th}$  and  $j^{th}$  row. Also, any fill-in entries appearing on the right hand side in (3) have already been updated at this point, and will not be changed subsequently. Hence, the resulting concentration matrix at the end of the second step of our algorithm lies in  $\mathcal{P}_{G_\sigma}$  (see Lemma 1 below for formal proof). The above construction by design also guarantees that  $\widehat{L}_{ij} = 0 = \widehat{L}_{ij}^D$  if  $i > j$ ,  $(i, j) \notin E_\sigma^D$ , and  $\widehat{L}_{ij} = \widehat{L}_{ij}^D$  if  $(i, j) \in E_\sigma$  or  $i = j$ , i.e., only the fill-in entries of  $\widehat{L}^D$  are changed.

We call the proposed statistical method Constrained Cholesky Approach (CCA) and the corresponding algorithm the CCA algorithm - see Algorithm 1 below. Note that  $\widehat{\Omega}$  (the resulting CCA estimate) is obtained in a fixed and finite number of steps, and there is no repetition of an identical sequence of steps until convergence. The following lemma (proof in Supplemental Section C) establishes that  $\widehat{\Omega}$  produced by CCA lies in  $\mathbb{P}_{G_\sigma}$ , i.e., it is positive definite and has the required pattern of zeros.

**Lemma 1** *Suppose  $n$  is greater than the largest clique size in  $G_\sigma^D$ . Let  $\widehat{\Omega}$  be the estimate of the concentration matrix produced by CCA method (see also Algorithm 1). Then  $\widehat{\Omega} \in \mathbb{P}_{G_\sigma}$ .*

**Remark 1** *The key idea used in the CCA algorithm is to first find a cover of the given graph for which a principled estimator can be easily computed (Step I), and then adjust the Cholesky values corresponding to the extra edges in the cover to obtain the desired sparsity in the precision matrix (Step II). This process works well for decomposable covers. A natural question to ask is whether there is some known class of graphs which would work even better, i.e., is the class of decomposable graphs maximal or optimal in some sense, or can we do better? We argue below that the proposed approach would either not work as effectively, or would even break down for other well-known classes of graphs studied in the graphical models literature. One candidate to consider is the class of homogeneous graphs (Letac and Massam [2007], Khare and Rajaratnam [2012]), which is a well-studied subclass of decomposable graphs. While the Gaussian MLE restricted to a homogeneous sparsity pattern is available in closed form, a homogeneous cover typically needs many more added edges compared to a decomposable cover. This would lead to many more fill-in entries, and hence increase the computational burden in Step II. Too many additional entries can also affect statistical precision. The same line of reasoning can be used to show that any special class of graphs which is a subset of the class of decomposable graphs (such as tress) would require additional edges, thus substantially increasing computational burden in Step II without any material benefit in Step I. On the other side, the class of Generalized Bartlett (GB) graphs (Khare et al. [2018]) contains the class of decomposable graphs as a special case. Unlike decomposable graphs, the Gaussian MLE for general GB graphs is not available in closed form. Hence, an iterative algorithm would be needed for Step I, which in turn would significantly increase computational burden. So, any gains and justification thereof for using a Generalized Bartlett cover would have to come from Step II, since there are fewer extra zeros to correct in the intermediate estimator of  $\Omega$ . However, these savings cannot reverse the substantial additional computational cost required for Step I. As the class of decomposable graphs is the maximal class of graphs for which the Gaussian MLE and its Cholesky factor can be obtained in closed form, any larger class of graphs (such as the GB class) would not be amenable to the proposed CCA approach. The above arguments underscore the correct balance that decomposable graphs achieve.*

Another question is whether the CCA estimators  $\widehat{\Omega}$  and  $\widehat{L}$  can be obtained as solutions to an optimization problem. Note that by definition the intermediate estimator  $\widehat{\Omega}^D$  in Step I above minimizes the negative Gaussian log-likelihood (subject to  $\Omega \in \mathbb{P}_{G_\sigma^D}$ ). Using the decomposability of  $G_\sigma^D$ , the intermediate Cholesky estimator  $\widehat{L}^D$  can thus be expressed as

$$\widehat{L}^D = \operatorname{argmin}_{L \in \mathbb{L}_{G_\sigma^D}} \{ \operatorname{tr}(LL^T S) - 2 \log |L| \}. \quad (4)$$

The next lemma (proof in Supplemental Section D) identifies the CCA estimator  $\widehat{L}$  obtained in Step II above as the unique solution to an optimization problem (given the intermediate estimator  $\widehat{L}^D$  obtained in Step I).

**Lemma 2** *Given the intermediate estimator  $\widehat{L}^D$ , the CCA estimator  $\widehat{L}$  uniquely minimizes (over the set  $\mathbb{L}_{G_\sigma}$ ) the function  $h(L) = \sum_{(i,j) \in E_\sigma \text{ or } i=j} (\widehat{L}_{ij}^D - L_{ij})^2$ .*

Since the intermediate estimator  $\widehat{L}^D$  is itself a solution to an optimization problem, the above lemma can be combined with (4) to obtain the following representation of the final CCA estimator.

**Lemma 3** *Given the sample covariance matrix  $S$ , the ordered graph  $G_\sigma$  and its filled graph  $G_\sigma^D$ , the final CCA estimator  $\widehat{L}$  can be expressed as*

$$\widehat{L} = \operatorname{argmin}_{L \in \mathbb{L}_{G_\sigma}} \sum_{(i,j) \in E_\sigma \text{ or } i=j} \left( \left( \operatorname{argmin}_{L \in \mathbb{L}_{G_\sigma^D}} \{ \operatorname{tr}(LL^T S) - 2 \log |L| \} \right)_{ij} - L_{ij} \right)^2.$$

The above lemma shows how CCA avoids an iterative optimization approach by decomposing the estimation problem into two steps. The first step projects the problem to a relevant space involving chordal graphs, and has a closed form solution. The second step projects this solution on to the desired space thus ensuring the correct sparsity pattern and preserving positive definiteness, and requires a single pass through the fill-in entries of  $\widehat{L}^D$ . These two steps together circumvent iterative/repetitive high-dimensional computations: a single iteration is all that is required at each of the two steps of CCA.

**Remark 2** *(Non-parametric interpretation of CCA) We now note that the intermediate estimator  $\widehat{L}^D$  can in fact be seen as a non-parametric estimator which does not rely on the Gaussian functional form. In particular, the corresponding precision matrix estimator  $\widehat{\Omega}^D = \widehat{L}^D(\widehat{L}^D)^T$  is the unique matrix in  $\mathbb{P}_{G_\sigma^D}$  which satisfies the constraint that the  $(i,j)^{\text{th}}$  entry of its inverse equals  $S_{ij}$  (the  $(i,j)^{\text{th}}$  entry of the sample covariance matrix) for every  $(i,j) \in E_\sigma^D$ . To see this more formally, as in Letac and Massam [2007], let  $I_{G_\sigma^D}$  be the linear space of symmetric incomplete matrices  $A$  with the  $(i,j)^{\text{th}}$ -entry missing for every  $(i,j) \notin E$ . Let  $Q_{G_\sigma^D}$  be the collection of all  $A \in I_G$  such that any submatrix of  $A$  corresponding to a maximal clique of  $G_\sigma^D$  is positive definite. For any  $A \in Q_{G_\sigma^D}$ , the decomposability of  $G_\sigma^D$  along with a result in Grone et al. [1984] implies the existence of a unique completion  $\tilde{A}$  of  $A$  such that  $\tilde{A}^{-1} \in \mathbb{P}_G$ . Now, let  $S^D$  denote the matrix in  $I_{G_\sigma^D}$  obtained by removing all entries with indices outside  $E_\sigma^D$ . If  $n$  is larger than the largest clique size in  $G_\sigma^D$ , then it follows that  $S^D \in Q_G$ . It now follows by [Letac and Massam, 2007, Theorem 2.1] that  $\widehat{\Omega}^D = (\tilde{S}^D)^{-1}$ . Note specifically that Step 1 on the CCA approach can be implemented without invoking the Gaussian functional form. As Lemma 2 demonstrates, the second step of the CCA*

approach (constructing the CCA estimator  $\hat{L}$  for  $\hat{L}^D$ ) is again non-parametric/distribution-free in nature and only adjusts the fill-in entries of  $\hat{L}^D$  to ensure that the CCA precision estimator lies in  $P_{G_\sigma}$ . Given the non-parametric flavor of the entire CCA procedure, the CCA estimator is more robust. It is thus more immune to outliers compared to the IPF and its variants which in turn fundamentally depend on the Gaussian likelihood.

---

Algorithm 1: The CCA Algorithm

---

INPUT - Sample covariance matrix  $S$   
 INPUT - Sparsity pattern encoded in a graph  $G$   
 Compute RCM fill reducing ordering  $\sigma$   
 Compute filled graph  $G_\sigma^D$   
 Compute Cholesky factor  $\hat{L}^D$  of  $\hat{\Omega}^D$  (as specified in (2))  
 Set  $\hat{L} \leftarrow \hat{L}^D$

```

for all  $i = 2$  to  $p$  do
  for all  $j = 1$  to  $i - 1$  do
    if  $(i, j) \notin E_\sigma$  then
      Set  $\hat{L}_{ij} = \frac{-\sum_{k=1}^{j-1} \hat{L}_{ik} \hat{L}_{jk}}{\hat{L}_{jj}}$ 
    end if
  end for
end for

```

OUTPUT - Return final estimates  $\hat{L}$  and  $\hat{\Omega} = \hat{L}\hat{L}^T$

---

### 3.2 Computational aspects of the CCA Algorithm

In this section, we provide relevant computational details and evaluate the computational complexity of each step in the CCA algorithm. (Algorithm 1). As part of calculating the computational complexity of the CCA algorithm, note the following.

- The complexity of the step to determine the RMC fill reducing ordering  $\sigma$  is  $O(|E_\sigma|)$  (see Chan and George [1980]).
- The complexity of computing  $G_\sigma^D$  (the decomposable cover) using the elimination tree method outlined in Section 2.5 is  $O\left(\sum_{j=1}^p n_j^2\right)$ , where  $n_j = \{i : 1 \leq j < i \leq p, (i, j) \in E_\sigma^D\}$  for every  $1 \leq j \leq p$ .
- Computational complexity of Step 1: The complexity of computing  $\hat{L}^D$  based on eq. (2) is calculated as  $O\left(p + \sum_{j=1}^p n_j^3\right)$ , since the complexity of computing the inverse of a matrix is the cube of the dimension of the matrix. Of course, it only makes sense to use (2) to compute  $\hat{L}^D$  if  $G_\sigma^D$  is sparse. For dense  $G_\sigma^D$  we can use a direct Cholesky

factorization to obtain  $\widehat{L}^D$  with complexity  $O(p^3)$ . As a practical rule, we use direct computation of  $\widehat{L}^D$  when  $|E_\sigma^D| > p^{5/3}$ , since in this case by Jensen's inequality

$$\sum_{j=1}^p n_j^3 \geq p \left( \frac{1}{p} \sum_{j=1}^p n_j \right)^3 = \frac{|E_\sigma^D|^3}{p^2} > p^3. \quad (5)$$

- Computational complexity of Step 2: The second step of obtaining  $\widehat{L}$  from  $\widehat{L}^D$  can be efficiently implemented by observing the following. Note that  $\widehat{\Omega} \in \mathbb{P}_{G_\sigma} \subseteq \mathbb{P}_{G^D}$ . Since  $G_\sigma^D$  is the filled graph for  $G_\sigma$ , it follows that  $\widehat{L}_{ij} = 0 = \widehat{L}_{ij}^D$  if  $i > j, (i, j) \notin E_\sigma^D$ . Also, by construction,  $\widehat{L}_{ij} = \widehat{L}_{ij}^D$  if  $(i, j) \in E_\sigma$  or  $i = j$ . Hence, the only entries which will be changed in the second step of Algorithm 1 are the fill-in entries or the edges in  $E_\sigma^D \setminus E_\sigma$ . The complexity of modifying these entries in the algorithm can be easily calculated as  $O(p|E_\sigma^D \setminus E_\sigma|)$ .

Straightforward calculations show that the complexities in the first two bullets are dominated by those in the last two bullets above, leading to the following lemma.

**Lemma 4 (Computational complexity of CCA)** *For any connected ordered graph  $G_\sigma$ , the computational complexity of the entire CCA algorithm is*

$$O \left( \min \left( p + \sum_{j=1}^p n_j^3 + p |E_\sigma^D \setminus E_\sigma|, p^3 \right) \right).$$

We now quantify the computational complexity of state-of-the-art methods. Recall that Iterated Proportional Fitting (IPF) is the classical “go-to method” for computing the MLE for  $\Omega$  in a Gaussian concentration graphical model when the underlying sparsity pattern (encoded in the graph  $G$ ) is known (Speed and Kiveri [1986]). In particular, the goal is to compute

$$\arg \min_{\Omega \in \mathbb{P}_G^+} \text{tr}(\Omega S) - \log \det(\Omega). \quad (6)$$

Note that each iteration of the IPF algorithm requires sequential conditional maximization of the Gaussian likelihood with respect to sub-matrices corresponding to maximal cliques of the given graph  $G$ . If a given maximal clique has  $c$  vertices, then the corresponding conditional maximization involves inversion of a  $(p-c)$ -dimensional matrix and thus requires  $O((p-c)^3)$  iterations. This can be expensive for sparse graphs where  $c \ll p$  in general. Several modifications of the original IPF algorithm which increase computational efficiency in such settings have been proposed over the last two decades. The line of work in Hara and Takemura [2010], Xu et al. [2011, 2012] and others focuses on ‘local’ updates of the clique based sub-matrices using triangulations and junction trees to avoid large matrix inversions. As pointed out in Xu et al. [2015], while these methods can significantly lower the amount of computations, they need significantly more memory. The IPSP method in Xu et al. [2015] employs the strategy of partitioning the set of maximal cliques of  $G$  into non-overlapping blocks, and then performing local updates for the clique sub-matrices in each block. All of the above methods are iterative and need an enumeration of the maximal cliques of the graph  $G$ . While such an enumeration can be done efficiently for some family of sparse graphs, it can also be very expensive in general and takes exponential time in the worst-case

Method	Overall complexity
CCA	$O\left(\min\left(p + \sum_{j=1}^p n_j^3 + p  E_\sigma^D \setminus E_\sigma , p^3\right)\right),$
G-IPF	$T_{Gl} \times O\left(\sum_{j=1}^p \tilde{n}_j^3 + p  E_\sigma \right)$
FIPF	$T_F \times O(p^2  E_\sigma )$
IPSP	$T_I \times O(p^2 \sum_{U \in \mathcal{U}}  U ) + T_{enum}$

Table 1: Overall computational complexity of various undirected/concentration graph model estimators (for connected  $G_\sigma$ ). For disconnected graphs, complexities can be computed over all the connected components and then added together. Here  $T_{Gl}, T_F, T_I$  denote the number of repetitions needed to achieve the convergence threshold for G-IPF, FIPF, IPSP respectively,  $T_{enum}$  is the time needed to enumerate the maximal cliques of  $G$ ,  $\tilde{n}_j = |\{i : 1 \leq i \leq p, (i, j) \in E_\sigma\}|$ ,  $n_j = |\{i : 1 \leq j < i \leq p, (i, j) \in E_\sigma^D\}|$ ,  $\mathcal{C}$  is the collection of all maximal cliques of  $G$ , and  $\mathcal{U}$  is a partition of the  $\mathcal{C}$ .

setting (see Example 5 below). In very recent work, Hojsgaard and Lauritzen [2023] cleverly employ a version of Woodbury’s identity in Harville [1977] to avoid enumeration of maximal cliques of  $G$  as well as large matrix inversions in the conditional maximization steps of the IPF algorithm. We refer to this algorithm, based on the “edgewise” and “covariance-based” version of IPF developed in Hojsgaard and Lauritzen [2023], simply as FIPF (Fast IPF).

An alternative approach to find the MLE in the Gaussian setting is described in [Hastie et al., 2009, Algorithm 17.1] and implemented in the *glasso* package. Essentially, this approach uses a modification of the well-known Glasso algorithm (i.e., without the  $\ell_1$  penalty term which accounts for the fact that the sparsity pattern in  $\Omega$  is known). We will refer to this algorithm as the G-IPF algorithm. Note that similar to the IPF and its adaptations, G-IPF repeats its iterations until an appropriate convergence threshold has been achieved. However, unlike these algorithms (except F-IPF), G-IPF does not require an enumeration of the maximal cliques of  $G$ . A straightforward analysis of [Hastie et al., 2009, Algorithm 17.1] and results in Xu et al. [2015], Hojsgaard and Lauritzen [2023] can be used to calculate the *overall* computational complexity of the IPSP, FIPF and G-IPF algorithms. These complexities, along with the complexity of the proposed CCA algorithm (based on the discussion at the beginning of this subsection) are summarized in Table 1.

The next lemma (proof in Supplemental Section E) compares the computational complexity of CCA with FIPF and IPSP.

**Lemma 5** (*Computational Complexity: CCA vs. FIPF and IPSP*) *For an arbitrary graph  $G$ , the computational complexity of even one iteration of the IPSP algorithm or the FIPF algorithm is greater than or equal to that of the entire CCA algorithm.*

The next lemma (proof in Supplemental Section F) compares the computational complexity of CCA with G-IPF especially in the context when  $p$  is large. To facilitate this analysis, we consider the class of  $p$ -vertex graphs with at least  $p^{5/3}$  edges, denoted by  $\mathcal{A}_p$ . This is a large class of graphs with elements ranging from *moderately sparse graphs* (since  $p^{5/3} = o(\binom{p}{2})$ ), as well as *very dense graphs* (with more than  $0.5\binom{p}{2}$  edges).

**Lemma 6** (*Computational Complexity: CCA vs. G-IPF*) *Consider the class  $\mathcal{A}_p$  of  $p$ -vertex graphs with more than  $p^{5/3}$  edges. Then*

- (a) For all graphs  $G \in \mathcal{A}_p$ , the CCA algorithm is computationally more efficient than even one iteration of the G-IPF algorithm.
- (b) The class of  $p$ -vertex graphs belonging to  $\mathcal{A}_p$  as a proportion of the total number of  $p$ -vertex graphs converges super-exponentially to 1 as  $p \rightarrow \infty$ . In particular,

$$\frac{|\mathcal{A}_p|}{2^{\binom{p}{2}}} \geq 1 - \sqrt{\frac{2}{\pi}} \exp(- (0.17p^2 - 3p^{5/3} \log p)) \text{ for } p \geq 100.$$

In summary, compared to competing methods the computational complexity of the proposed CCA method is always lower for any dimension (when compared to FIPF and IPSP) or almost always lower (when compared to G-IPF) as the dimension  $p$  gets larger, underscoring its direct relevance in modern settings. Equally or more importantly, this lower complexity is for a single iteration, bearing in mind that CCA requires only one iteration, while competing methods require many. These two properties together make a very strong and compelling case for the use of CCA in modern settings.

We now turn to comparing the CCA and G-IPF approaches in the sparse graph setting (graphs with less than  $p^{5/3}$  edges). Though a general comparison of the computational complexities of CCA and G-IPF is not available in this setting, important insights can be obtained through a case-by-case analysis. Recall that a single iteration of the G-IPF algorithm has complexity of the order  $\sum_{j=1}^p \tilde{n}_j^3 + p|E_\sigma|$ , while the single and *only* iteration of Algorithm 1 has computational complexity of the order  $\sum_{j=1}^p n_j^3 + p + p|E_\sigma^D \setminus E_\sigma|$  for adequately sparse graphs. Since the G-IPF algorithm does not use the filled graph  $G_\sigma^D$ , comparing  $|E_\sigma|$  and  $|E_\sigma^D \setminus E_\sigma|$  (also  $\tilde{n}_j$  and  $n_j$ ) is not straightforward and hence general results comparing these quantities are not available. However, we are able to compare these quantities (and consequently the computational complexities of CCA vs. G-IPF, and those of FIPF and IPSP) in some key examples in the next subsection.

### 3.3 Examples and illustrations

*Example 1 (grid)* An  $a \times b$  grid is a common sparse non-decomposable graph with  $p = (a+1)(b+1)$  vertices. For the default column-based ordering  $\sigma$  (depicted in Figure 1 (middle) with  $a = b = 3$ ) the filled graph  $G_\sigma^D$  can be obtained by adding a NE-SW diagonal in each of the  $ab$  unit squares in the grid. The RCM ordering (Figure 1, right) again leads to the same NE-SW diagonals as fill-in edges. For the default row-based ordering  $\sigma$  (depicted in Figure 2 (left) with  $a = b = 3$ ) the filled graph  $G_\sigma^D$  can be obtained by adding a NW-SE diagonal in each of the  $ab$  unit squares in the grid. It is important to note that the orientation of these additional diagonals depends on the imposed ordering  $\sigma$ . For example, if we add diagonals with a NW-SE orientation, then the resulting graph does not admit the column-based ordering in Figure 1 (middle) as a perfect vertex elimination scheme. In general, adding diagonals with different orientations in each unit square of the grid may not lead to a decomposable graph (see Figure 2 (right) for an example). An example where adding diagonals of different orientations leads to a decomposable graph is provided in Figure 2 (middle), and a corresponding perfect vertex elimination scheme is also provided.

Let  $\sigma$  be the RCM ordering depicted in Figure 1 (right). In this case, straightforward

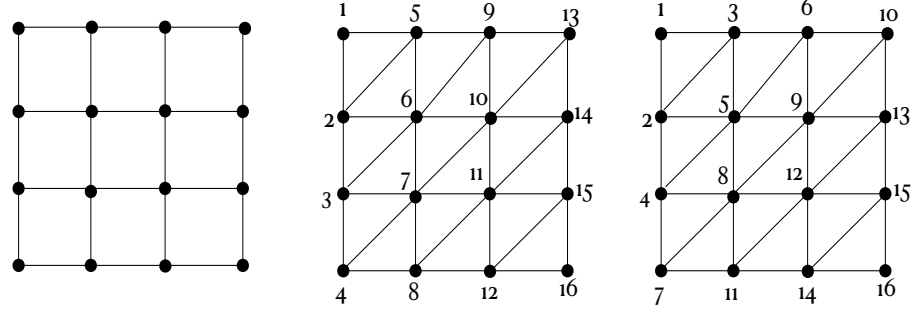


Figure 1: (left) A  $3 \times 3$  grid with 16 vertices. (middle) Filled graph for column-based ordering of vertices with added diagonals in NE-SW orientation. (right) Filled graph for RCM ordering.

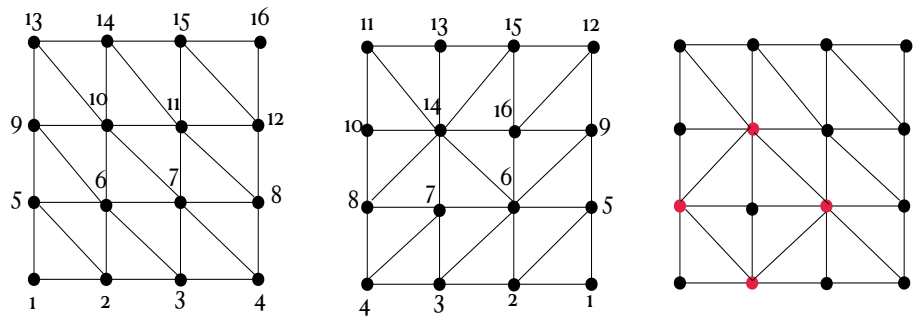


Figure 2: (left) Filled graph for row-based ordering of vertices with added diagonals in NW-SE orientation. (middle) An example when adding diagonals of different orientations leads to a decomposable graph, and the corresponding perfect vertex elimination ordering. (right) An example when adding diagonals of different orientations does not lead to a decomposable graph, as the induced subgraph on the highlighted vertices is a 4-cycle.

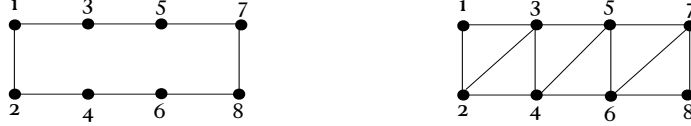


Figure 3: An 8-cycle with RCM ordering of vertices (left), corresponding filled graph (right).

computations show that

$$|E_\sigma^D \setminus E_\sigma| = ab < 2ab + a + b = |E_\sigma|$$

and

$$\sum_{j=1}^p n_j^3 = 27ab + a - 11b < 64ab - 10a - 10b - 12 = \sum_{j=1}^p \tilde{n}_j^3.$$

In this case the CCA algorithm and a single iteration of the G-IPF algorithm both have complexity  $O(p^2)$ . Also, the underlying graph has  $O(p)$  maximal cliques of size 2, and it follows from Table 1 that both FIPF and IPSP have computational complexity  $O(p^3)$  in this case.

With the above comparisons in mind, in modern environmental and earth science applications, there is a compelling need to model covariates on a spatial grid and their corresponding dependencies in a sparse manner. In particular, the sparse modeling of partial correlations (and conditional independences) on a grid has been shown to be highly effective in modern climate and paleo-climate applications. In such applications the dimension can be much larger than the available sample size (see Guillot et al. [2015]). Here the goal is to not just estimate a sparse Markov Random Field, but it is critically important to also quantify the uncertainty inherent to such estimation, through resampling or other methods (see Guillot et al. [2015]). When estimation is not in closed form, quantifying uncertainty through multiple bootstrap estimations of the inverse covariance matrix can be extremely computationally prohibitive. The grid example above thus demonstrates direct applicability of the proposed CCA method in a contemporary application domain.

*Example 2 (cycle).* The  $p$ -cycle is another standard example of a sparse non-decomposable graph. A simple induction argument shows that  $|E_\sigma^D \setminus E_\sigma| = p - 3 < p = |E_\sigma|$  if  $\sigma$  is chosen to be the RCM fill reducing ordering of the vertices (see Figure 3). In this case,  $\tilde{n}_j = n_j = 2$  for every  $1 \leq j \leq p - 1$ ,  $\tilde{n}_p = 2$  and  $n_p = 0$ . Hence,  $\sum_{j=1}^p n_j^3 < \sum_{j=1}^p \tilde{n}_j^3$ . Hence, both the CCA and one iteration of G-IPF have complexity  $O(p^2)$  in this case. When considering the competing methods of FIPF and IPSP, note that since a  $p$ -cycle has  $p$  maximal cliques of size 2, it follows from Table 1 that both these methods have per iteration computational complexity  $O(p^3)$  in this case. The IHT algorithm in Xu et al. [2011] has a complexity of  $O(p)$  (per iteration) in this case. However, as mentioned in Xu et al. [2015], this algorithm can be prohibitively memory intensive in general.

*Example 3 (almost complete graph).* The largest/densest non-decomposable graph with  $p$  vertices can be obtained by taking a complete graph (with  $\sigma$  being the identity permutation),

and removing the edges  $(p, p-2)$  and  $(p-1, p-3)$ . Then the induced subgraph on the subset of vertices  $\{p, p-1, p-2, p-3\}$  is a 4-cycle, which implies  $E_\sigma$  is not a decomposable graph. In this case, the filled graph  $E_\sigma^D$  can be obtained by adding the edge  $(p, p-2)$  to  $E_\sigma$ . In this dense case, the computational complexity of CCA, based on the discussion corresponding to eq. (5), is  $O(p^3)$ . On the other hand for G-IPF,

$$\sum_{j=1}^p n_j^3 = \sum_{k=1}^{p-1} k^3 - (3^3 - 2^3) = \frac{(p-1)^2 p^2}{4} - 19,$$

which implies that the computational complexity of one iteration of G-IPF is  $O(p^4)$ : an entire order of magnitude larger. When considering FIPF and IPSP, note that the underlying graph has four maximal cliques of size  $p-2$ . Hence, the computational complexity of both FIPF and IPSP (per iteration) is  $O(p^3)$  by Table 1.

*Example 4 (Bipartite graph).* Consider a bipartite graph setting, where  $V = A \uplus B$  with  $|A| = m$  and  $|B| = p - m$ , and  $(u, v) \in E$  if and only if  $u \in A, v \in B$  or  $u \in B, v \in A$ . We assume without loss of generality that  $m \leq p/2$ . For this non-decomposable graph, consider any vertex ordering  $\sigma$  which assigns labels  $\{p, p-1, \dots, p-m+1\}$  to vertices in  $A$ , and the remaining labels to vertices in  $B$ . Such an ordering can be converted to an RCM ordering with just one change to the vertex labels, but we consider the above partition based ordering for simplicity of exposition. In this case,  $G_\sigma^D$  can be obtained by adding edges so that each vertex in  $A$  shares an edge with all other vertices in  $A$ . In particular,  $|E_\sigma^D \setminus E_\sigma| = \binom{m}{2}$ . It follows that  $n_j = m$  for  $1 \leq j \leq p-m$ , and  $n_j = p-j$  for  $j > m$ . On the other hand  $\tilde{n}_j = p-m$  for  $1 \leq j \leq m$  and  $\tilde{n}_j = m$  for  $j > m$ . Consider the ‘sparse’ case, when  $m = o(p^{2/3})$  and  $\hat{L}^D$  is computed using (2). In this case, note that

$$p + \sum_{j=1}^p n_j^3 + p|E_\sigma^D \setminus E_\sigma| = (p-m)m^3 + \sum_{j=1}^m j^3 + p + pm^2 \leq Cpm^3$$

Since  $p/2 < p-m < p$ , it follows that the computational complexity of CCA is  $O(pm^3)$ . Similarly, note that

$$\sum_{j=1}^p \tilde{n}_j^3 + p|E_\sigma| = (p-m)m^3 + m(p-m)^3 + pm(p-m)$$

which implies that the computational complexity of G-IPF (per iteration) is  $O(mp^3)$ . Now let us consider the other competing methods FIPF and IPSP. Since there are  $m(p-m)$  maximal cliques, each of size 2, it follows that the computational complexity of FIPF and IPSP is  $O(mp^3)$  as well. Since  $m = o(p^{2/3})$ , we conclude that the computational complexity of the entire CCA algorithm is an order of magnitude smaller than the per iteration complexity of the other three algorithms. In the ‘dense’ case where  $m$  is at least  $p^{2/3}$ , and  $\hat{L}^D$  is computed using the usual Cholesky factorization approach, the complexity of CCA is  $O(p^3)$ , while the complexity for the competing methods is at least  $O(p^{3+2/3})$ .

*Example 5 (Multipartite graph - exponential number of cliques).* Consider a setting, where  $p = 3m$ ,  $V = \uplus_{i=1}^m A_i$  with each  $A_i$  having 3 vertices, and  $(u, v) \in E$  if and only if  $u \in A_k, v \in A_{k'}$  for  $k \neq k'$ . Consider any ordering  $\sigma$  which assigns labels  $\{3i-2, 3i-1, 3i\}$  to vertices

Non-decomp. graph	Sparsity	CCA	G-IPF	FIPF	IPSP
Grid	Sparse	<b><math>O(p^2)</math></b>	$T_G \times O(p^2)$	$T_F \times O(p^3)$	$T_I \times O(p^3)$
Cycle	Sparse	<b><math>O(p^2)</math></b>	$T_G \times O(p^2)$	$T_F \times O(p^3)$	$T_I \times O(p^3)$
Bipartite ( $m, p-m$ ) partition	Sparse	<b><math>O(pm^3)</math></b>	$T_G \times O(mp^3)$	$T_F \times O(pm^3)$	$T_I \times O(pm^3)$
	Dense	<b><math>O(p^3)</math></b>	$T_G \times \Omega(p^{11/3})$	$T_F \times \Omega(p^{11/3})$	$T_I \times \Omega(p^{11/3})$
Almost complete	Dense	<b><math>O(p^3)</math></b>	$T_G \times O(p^4)$	$T_F \times O(p^3)$	$T_I \times O(p^3)$
Multipartite exponential # cliques	Dense	<b><math>O(p^3)</math></b>	$T_G \times O(p^4)$	$T_F \times e^{O(p)}$	$T_I \times e^{O(p)}$

Table 2: Computational complexity comparison of CCA with other competing methods for some key non-decomposable graphs. For iterative methods, the complexity of a single iteration is multiplied with the total number of iterations ( $T_G$  for G-IPF,  $T_F$  for FIPF,  $T_I$  for IPSP). The lowest computational complexity for each row is highlighted in bold.

in  $A_i$  for  $1 \leq i \leq m$ . This is a dense graph with  $\binom{p}{2} - p$  edges, and the computational complexity of CCA is  $O(p^3)$ . Since  $\tilde{n}_j = p - 2$  for every  $j$ , it follows that the computational complexity of G-IPF (per iteration) is  $O(p^4)$ . With regards to the other two methods FIPF and IPSP, there are an exponential number of maximal cliques ( $3^{p/3}$  in particular), and hence the computational complexity of these methods (per iteration) is exponential in  $p$ .

For comparison purposes, the results in the examples above are summarized in Table 2. The analysis above facilitates a detailed understanding of the properties of the proposed CCA method. In particular, the computational advantages of the proposed CCA algorithm stem from three properties: (a) G-IPF, FIPF and IPSP have to repeat their iterations  $T$  times, while no such repetition is necessary for the CCA method, (b) FIPF and IPSP (not G-IPF though) require an enumeration of the maximal cliques of the graph  $G$ , which can be expensive, especially for moderately sparse or dense graphs, and (c) in a large majority of settings, even a single iteration of the CCA algorithm is in general computationally more efficient than even a single iteration of the G-IPF and other algorithms. Together, these three properties contribute to the significant computational advantage of the CCA approach.

## 4 High-dimensional asymptotic properties

In this section we examine the large sample properties of the proposed estimators in a high-dimensional setting. Consider once more the setting in Section 3. We will allow the number of variables  $p = p_n$  to increase with the sample size  $n$ . We consider a true data generating model under which i.i.d. observations  $\mathbf{Y}_{n,1}, \dots, \mathbf{Y}_{n,n} \in \mathbb{R}^{p_n}$  are generated from a distribution with mean  $\mathbf{0}$  and precision matrix  $\bar{\Omega}_n \in \mathbb{P}_{p_n}^+$  for every  $n \geq 1$ . In other words,  $\{\bar{\Omega}_n\}_{n \geq 1}$  denote the sequence of true inverse covariance matrices. Let  $\{\bar{L}_n\}_{n \geq 1}$  denote the corresponding sequence of Cholesky factors of  $\bar{\Omega}_n$ , and let  $\{\bar{\Sigma}_n\}_{n \geq 1}$  denote the corresponding sequence of true covariance matrices. The graph  $G = G_n$  encodes the sparsity pattern in  $\bar{\Omega}_n$ ,  $\sigma = \sigma_n$  denotes a given fill-reducing ordering for  $G$ , and  $G_\sigma^D$  denotes the corresponding filled graph. Let  $\bar{P}$  denote the probability measure underlying the true data generating model described above.

We now introduce some quantities related to  $G_\sigma$  and  $G_\sigma^D$  which will be needed for specifying the convergence rate of the CCA based estimators. Let  $a_n^D$  denote the product of the

maximum number of non-zero entries in any column of  $\bar{L}_n$  and the maximum number of non-zero entries in any row of  $\bar{L}_n$ . In particular

$$a_n^D = \left( 1 + \max_{1 \leq j \leq p-1} |\{u > j : (u, j) \in E_\sigma^D\}| \right) \times \left( 1 + \max_{2 \leq i \leq p} |\{u < i : (i, u) \in E_\sigma^D\}| \right).$$

The quantity  $\tilde{a}_n^D$  is similarly defined below, although focusing exclusively on the fill-in entries only as opposed to the entire filled graph. In particular

$$\tilde{a}_n^D = \left( \max_{1 \leq j \leq p-1} |\{u > j : (u, j) \in E_\sigma^D \setminus E_\sigma\}| \right) \times \left( \max_{2 \leq i \leq p} |\{u < i : (i, u) \in E_\sigma^D \setminus E_\sigma\}| \right).$$

Let  $c = |E_\sigma^D \setminus E_\sigma|$  be the number of fill-in entries. These fill-in entries can be ordered based on the traversal path described in Step II of the CCA algorithm. For every  $1 \leq r \leq c$ , let  $\mathcal{F}_r^D$  denote the collection of previous fill-in entries which contribute to the computation of the  $r^{th}$  fill-in entry in Algorithm 1, see RHS of (3). In particular if the  $r^{th}$  fill-in entry is  $(i, j)$ , then

$$\begin{aligned} \mathcal{F}_r^D = & \left\{ \tilde{r} : 1 \leq \tilde{r} \leq r, \exists k < j < i \text{ such that } \tilde{r}^{th} \text{ fill-in entry is } (j, k) \text{ with } (i, k) \in E_\sigma^D \right\} \\ & \uplus \left\{ \tilde{r} : 1 \leq \tilde{r} \leq r, \exists k < j < i \text{ such that } \tilde{r}^{th} \text{ fill-in entry is } (i, k) \text{ with } (j, k) \in E_\sigma^D \right\}. \end{aligned}$$

We now state two of the three assumptions that are needed for our asymptotic results. Both of these assumptions are quite standard in the high-dimensional asymptotic literature.

- (A1 - Bounded Eigenvalues) There exists  $\delta > 0$  (not depending on  $n$ ) such that  $0 < \delta \leq \lambda_{\min}(\bar{\Omega}) \leq \lambda_{\max}(\bar{\Omega}) \leq \delta^{-1} < \infty$ .
- (A2 - Sub Gaussianity) The random vectors  $\mathbf{Y}_{n,1}, \dots, \mathbf{Y}_{n,n}$  are sub-Gaussian i.e., there exists a constant  $c > 0$  such that for every  $\mathbf{x} \in \mathbb{R}^p$ ,  $E[e^{\mathbf{x}'\mathbf{Y}^i}] \leq e^{c\mathbf{x}'\mathbf{x}}$ . Along with Assumption A1, this in particular implies that the sub-Gaussian norm of  $\boldsymbol{\alpha}^T \mathbf{Y}^i$ , for any  $\boldsymbol{\alpha}$  with  $\boldsymbol{\alpha}^T \boldsymbol{\alpha} = 1$ , is uniformly bounded by a constant  $\kappa$ .

Assumption A1 states that the eigenvalues of the sequence of true covariance matrices are uniformly bounded. As mentioned above, these are standard assumptions in high-dimensional covariance asymptotics, see Bickel and Levina [2008a], Rothman et al. [2008], Peng et al. [2009], Xiang et al. [2015]. Before stating the third required assumption, we define a function  $g^D$  which maps  $\{1, 2, \dots, c\}$  to  $\mathbb{R}_+$  recursively as follows.

$$g^D(1) = \frac{6}{\delta} \text{ and } g^D(r) = \frac{3}{\delta} \sum_{\tilde{r} \in \mathcal{F}_r^D} g^D(\tilde{r})$$

for  $2 \leq r \leq c$ . This function is critical in capturing the propagation of errors while modifying the fill-in entries to compute the CCA Cholesky estimate  $\hat{L}$  from  $\hat{L}^D$ . The third required assumption stipulates that  $p$  increases with  $n$  at an appropriate sub-exponential rate depending on the graph based quantities defined above.

- (A3 - Growth rate for  $p_n$ )  $\frac{s_{CCA} \log p}{n} \rightarrow 0$  as  $n \rightarrow \infty$ , where

$$s_{CCA} = \min \left( a_n^D, |E_\sigma^D| + 1 \right) \tilde{a}_n^D \left( 1 + \max_{1 \leq r \leq c} g^D(r) \right)^2.$$

With the required assumptions and notation in hand, we establish our consistency result for CCA. Part (a) of the result establishes bounds for the intermediate estimator  $\hat{L}^D$ , and part (b) established bounds for the final CCA estimators  $\hat{L}$  and  $\hat{\Omega}$ .

**Theorem 1** (*Convergence rates for CCA*) *Suppose that assumptions A1-A3 are satisfied. Then the following results hold.*

(a) *There exists a constant  $K^*$  such that*

$$\bar{P} \left( \left\| \hat{L}^D - \bar{L} \right\|_2 \leq K^* \sqrt{\frac{\min(a_n^D, |E_\sigma^D| + 1) \log p}{n}} \right) \rightarrow 1 \text{ as } n \rightarrow \infty.$$

(b) *There exist constants  $K$  and  $K'$  such that*

$$\bar{P} \left( \left\{ \left\| \hat{L} - \bar{L} \right\|_2 \leq K \sqrt{\frac{s_{CCA} \log p}{n}} \right\} \cap \left\{ \left\| \hat{\Omega} - \bar{\Omega} \right\|_2 \leq K' \sqrt{\frac{s_{CCA} \log p}{n}} \right\} \right) \rightarrow 1 \text{ as } n \rightarrow \infty.$$

Like IPF, our work/model assumes that the graph  $G$  is known. When it is not known, it can be constructed using thresholding methods for sparse inverse covariance estimates as in Hero and Rajaratnam [2012] or Zhang et al. [2021].

**Remark 3** (*Weak convergence in the fixed  $p$  setting*) *When  $p$  does not vary with  $n$ , distributional convergence results which show that  $\hat{\Omega}$  is  $\sqrt{n}$ -consistent for  $\bar{\Omega}$  can be established under mild moment assumptions. In particular, assume that the underlying distribution  $F$  of the i.i.d. observations  $\mathbf{Y}_1, \mathbf{Y}_2, \dots, \mathbf{Y}_n$  satisfies the assumption  $\int_{\mathbb{R}^p} \prod_{i=1}^p |x_i|^{a_i} dF(\mathbf{x}) < \infty$ , where  $a_1, a_2, \dots, a_p$  are non-negative integers which satisfy  $\sum_{i=1}^p a_i = 4$ . Under this assumption, it can be shown that  $\sqrt{n}(\hat{\Omega} - \bar{\Omega})$  converges to a multivariate Gaussian limit as  $n \rightarrow \infty$  (see Supplemental Section B).*

## 4.1 Comparison with operator norm convergence rate for graphical Gaussian MLE

High-dimensional convergence rates for the graphical Gaussian MLE (solution of (6)) are not directly available in the current literature. However, minor modifications to the argument in [Rothman et al., 2008, Theorem 1] lead to a Frobenius norm convergence rate of  $\sqrt{\frac{(1+|E_\sigma|) \log p}{n}}$  for the graphical Gaussian MLE, under Assumptions A1-A2 (and a modified Assumption A3 which states that  $\sqrt{\frac{(1+|E_\sigma|) \log p}{n}} \rightarrow 0$  as  $n \rightarrow \infty$ ). Since the Frobenius norm dominates the operator norm, the above rate of  $\sqrt{\frac{(1+|E_\sigma|) \log p}{n}}$  also applies to the operator norm. To our knowledge, this is the best available operator norm convergence rate for the constrained Gaussian MLE (with a general graph  $G$ ). Hence, the comparison between the available operator norm convergence rates for the CCA and the graphical Gaussian MLE reduces to the comparison between the order of the quantities  $s_{CCA}$  and  $|E_\sigma|$ .

Note that  $s_{CCA}$  is a product of two factors:  $\min(a_n^D, |E_\sigma^D| + 1)$  (corresponding to Step I of Algorithm 1) and  $\tilde{a}_n^D (1 + \max_{1 \leq r \leq c} g^D(r))^2$  (corresponding to Step II of Algorithm 1). We are able to obtain the term  $\min(a_n^D, |E_\sigma^D| + 1)$  (instead of just  $|E_\sigma^D| + 1$ ) in the operator norm

bounds because the intermediate estimators  $\hat{L}^D$  and  $\hat{\Omega}^D$  are available in closed form. While  $|E_\sigma^D| > |E_\sigma|$  for all ordered graphs, in many settings  $a_n^D$ , the product of the maximum number of non-zero entries in any row of  $\bar{L}$  and the maximum number of non-zero entries in any column of  $\bar{L}$ , is of a lower order than  $|E_\sigma|$ . Hence, if the multiplicative factor corresponding to Step II does not grow too fast,  $s_{CCA}$  can be of a lower order than  $|E_\sigma|$ . To summarize, key properties of the CCA approach – (i) the availability of the intermediate estimator in closed form, and (ii) the final estimator requiring a finite number of tractable algebraic changes to the intermediate estimator – together allow us to directly analyze the operator norm of the estimation error and establish corresponding rates. Importantly, we have a high-dimensional setting where better computational properties of the CCA approach translate to, and are directly relevant for, establishing better statistical properties. In this sense, these two properties are complementary. Note that the graphical Gaussian MLE however does not readily allow convergence in the operator norm, forcing existing analyses to target the Frobenius norm of the estimation error. The corresponding rates for the Frobenius norm are then borrowed for the operator norm, leading to looser bounds in high-dimensional settings.

While a general comparison of  $s_{CCA}$  and  $|E_\sigma|$  is not available, we undertake a comparison in some of the key examples considered at the end of Section 3.2. It turns out that in most of these examples,  $s_{CCA}$  is of a smaller (or same) order as  $|E_\sigma|$ . We now consider the five classes of graphs from Section 3.3, and compare the available statistical accuracy rates of the CCA algorithm with that of the graphical Gaussian MLE for each of these classes.

*Example 1 (grid) contd.* Consider an  $a \times b$  grid with  $p = (a+1)(b+1)$  vertices. If  $\sigma$  is the RCM fill reducing ordering (see Figure 1, right), then the maximum number of non-zero entries in any row or column of  $\bar{L}$  is 4, which implies that  $\min(a_n^D, |E_\sigma^D|) = O(1) \ll 2ab + a + b = |E_\sigma|$ . In this case  $\mathcal{F}_r^D = \emptyset$  for every  $1 \leq r \leq c$ , which implies that the second multiplicative factor for  $s_{CCA}$  is  $O(1)$ . Hence  $s_{CCA} = O(1)$  is an order of magnitude smaller than  $|E_\sigma| = O(p)$ .

*Example 2 (cycle) contd.* If  $\sigma$  is the RCM fill reducing ordering (see Figure 3), it then follows that the maximum number of non-zero entries in any row or column of  $\bar{L}$  is bounded by 4, hence  $a_n^D = O(1)$ , and  $\min(a_n^D, |E_\sigma^D|) = O(1) \ll p = |E_\sigma|$ . However, the second multiplicative factor for  $s_{CCA}$  turns out to be exponential in  $p$ . In this case,  $c = p - 3$ , and straightforward calculations show that  $\max_{1 \leq r \leq c} g^D(r) = g^D(c) = O((3\delta^{-1})^{p-4})$  (see Assumption A1 above). Hence, overall  $|E_\sigma|$  is of a much smaller order than  $s_{CCA}$ . We show however that through more targeted arguments specific to the  $p$ -cycle setting, and an additional constraint on  $\bar{L}$ , a significantly better convergence rate than  $\sqrt{s_{CCA} \log p/n}$  can be obtained for the CCA estimator. In particular, for proving such a result, Assumption A3 above needs to be replaced by the following assumption.

- (A3') The quantity  $\max_{3 \leq j \leq p-1} \frac{|\bar{L}_{j,j-2}|}{\bar{L}_{jj}}$  is uniformly (in  $n$ ) bounded away from 1, and  $\frac{|E_\sigma| \log p}{n} \rightarrow 0$  as  $n \rightarrow \infty$ .

The first part of Assumption A3' essentially constrains the non fill-in entry in most rows of  $L_0$  to be smaller in magnitude than the corresponding diagonal entry. The following lemma now establishes a Frobenius norm convergence rate for the CCA estimator that matches the Frobenius norm convergence rate for the graphical Gaussian MLE. The proof of this lemma is provided in the Supplemental material at the end of the paper.

**Lemma 7** (*Improved CCA bounds for  $p$ -cycle*) *Consider the setting where  $G_\sigma = (V, E_\sigma)$  is a  $p$ -cycle equipped with the RCM based fill reducing ordering illustrated in Figure 3. Then,*

under Assumptions A1, A2 and A3', there exist constants  $\tilde{K}$  and  $\tilde{K}'$  such that the estimators  $\hat{L}$  and  $\hat{\Omega}$  satisfy

$$\bar{P} \left( \left\{ \left\| \hat{L} - \bar{L} \right\|_F \leq \tilde{K} \sqrt{\frac{(|E_\sigma| + 1) \log p}{n}} \right\} \cap \left\{ \left\| \hat{\Omega} - \bar{\Omega} \right\|_F \leq \tilde{K}' \sqrt{\frac{(|E_\sigma| + 1) \log p}{n}} \right\} \right) \rightarrow 1$$

as  $n \rightarrow \infty$ .

*Example 3 (almost complete graph) contd.* In this case both  $\min(a_n^D, |E_\sigma^D|)$  and  $|E_\sigma|$  are of order  $p^2$ , and since there is only fill-in entry ( $c = 1$ ), it follows that the second multiplicative factor for  $s_{CCA}$  is  $O(1)$ . Hence, in this case both  $s_{CCA}$  and  $|E_\sigma|$  are of order  $p^2$ .

*Example 4 (Bipartite graph) contd.* Consider a bipartite graph with sets  $A$  and  $B$  forming a partition of the vertex set  $V$ , such that  $|A| = m$  and  $|B| = p - m$  with  $m = O(1)$ . Consider the ordering  $\sigma$  as defined in Section 3.2 for this setting. In this case both  $\min(a_n^D, |E_\sigma^D|)$  and  $|E_\sigma|$  are of order  $p$ . Again, since  $c = \binom{m}{2} = O(1)$ , it follows that the second multiplicative factor for  $s_{CCA}$  is  $O(1)$ . Hence, in this case both  $s_{CCA}$  and  $|E_\sigma|$  are of order  $p$ .

*Example 5 (Multipartite graph) contd.* In this case, both  $\min(a_n^D, |E_\sigma^D|)$  and  $|E_\sigma|$  are of order  $p^2$ . Since fill-in edges are only allowed within each 3-element partition sets  $A_i$ , it can be shown that  $\max_{1 \leq r \leq c} g^D(r)$  and  $\tilde{a}_n^D$  are  $O(1)$ . To conclude,  $s_{CCA}$  and  $|E_\sigma|$  are both order  $p^2$ .

In summary, the examples above demonstrate that except in settings when the underlying graphs are highly sparse (such as cycles), the proposed CCA approach has demonstrably better statistical performance than the MLE (in terms of best available operator norm convergence rate) for moderately sparse and dense graphs. This combined with its superior computational complexity suggests that in modern high-dimensional settings, the CCA approach should be the preferred method. The only exceptions are cases when the underlying graph is a cycle or a graph close to a cycle.

## 5 Numerical Illustrations and real data applications

### 5.1 Simulation experiment: evaluation of CCA when $G$ is given

In this section, we evaluate the high-dimensional empirical performance of the CCA algorithm in a simulation setting where the underlying graph  $G$  is assumed to be given/known. Against the backdrop of the results on computational complexity in Section 3.2 (Lemma 5, Lemma 6 and Table 1) we compare the performance of the CCA algorithm and the G-IPF algorithm. For each value of  $p \in \{500, 1000, 1500, 2000, 5000\}$ , the following procedure is repeated: The true  $\Omega$  has a random sparsity pattern of approximately  $2p$  edges. To generate  $\Omega = L^t L$  for a given  $p$ , we initially generate  $L$ , a lower triangular matrix, in the following manner: Randomly select some entries of  $L$  to be zero (approximately less than  $2p$ ). Amongst these we randomly set half of them to be positive and the other half to be negative. In addition, the off-diagonal entries of  $L$  are drawn from the uniform distribution over  $[0.3, 0.7]$ . Finally, we choose the diagonal entries from the uniform distribution over  $[2, 5]$ . The sample size takes values as follows:  $n = \{0.5p, 0.75p, p, 2p\}$ . We generate 50 datasets for each of these settings from both the multivariate Gaussian and the heavy-tailed multivariate- $T$  distribution with 3 degrees of freedom.

For the Gaussian case, both the CCA algorithm and the G-IPF algorithm are then used to obtain estimates of  $\Omega$ . We also present results from a hybrid approach, which uses the CCA estimate as the initial estimate in G-IPF as opposed to the diagonal matrix with diagonal entries  $\{1/S_{ii}\}_{i=1}^p$ . The results presented below are the average relative Frobenius norm estimation errors ( $\frac{\|\hat{\Omega} - \Omega\|}{\|\Omega\|}$ ) over the 50 datasets generated for each sample size and underlying distribution. The results of the simulations for the multivariate Gaussian case are provided in Table 3. CCA produces significantly better wall-times compared to G-IPF without compromising on accuracy.

For the multivariate- $T$  datasets, we compare the performance of the CCA algorithm to G-IPF, and the *tlasso-IPF* algorithm from [Feingold and Drton, 2011, Section 3.2]. The results are provided in Table 4. The results show that the scalability of the CCA algorithm is even more pronounced compared to G-IPF in the heavy-tailed  $T$ -distribution case. Note that the *tlasso-IPF* uses the EM algorithm to obtain maximum likelihood estimates of concentration matrices (with a given sparsity pattern) assuming that the underlying data is generated from a multivariate- $t$  distribution. It is a double iterative algorithm, as the M-step in each iteration of the EM algorithm involves the iterative IPF algorithm. The maximum number of iterations for the EM algorithm was set to 100, and for the IPF algorithm was set to 1000. We report an “N/A” for estimation error values of the iterations for a given setting which does not finish in 4 days. For  $p = 2000$  and 5000, this is the case for the *t-lasso* algorithm. For lower values of  $p$ , the time taken by *t-lasso* is anywhere between 500 to 2000 times more as compared to the CCA algorithm. The estimation error for the resulting estimates is still very high, which suggests that more iterations are needed for convergence of the EM algorithm. To summarize, the results in Tables 3 and 4 demonstrate how state-of-the-art iterative algorithms can be prohibitively expensive in high-dimensional settings, and provide compelling reasons to use the proposed non-iterative CCA algorithm for fast and accurate estimation in modern high-dimensional applications.

## 5.2 Simulation experiment: evaluation of CCA when $G$ is not given

In practice, the graph  $G$  is not given/known. In this setting, a graph selection step is required prior to CCA, and we use the *FST* method [Zhang et al., 2021] for this purpose. *FST* is a non-iterative thresholding method (extending ideas in Rothman et al. [2009]) that is scalable to ultra high-dimensional settings, and is also theoretically supported by high-dimensional statistical consistency results (see Section 5 of Zhang et al. [2021] for details). However, the sparse estimate of  $\Omega$  provided by *FST* is not guaranteed to be positive definite. Setting  $G$  as the sparsity pattern in  $\Omega$  estimated by *FST*, and then applying the proposed CCA method in Section 3 yields a positive definite estimate of  $\Omega$  with exactly the same sparsity pattern as the *FST* estimate of  $\Omega$ . We refer to this approach as *FST+CCA*. The *FST* based estimate of  $G$  can have several connected components, in which case the CCA method is separately applied on each component. Doing so enables us to use techniques such as sparse matrix representation and parallel computation to gain efficiency.

We compare the *FST+CCA* method to two leading methods: Glasso and BigQUIC. These two are state-of-the-art penalized likelihood methods for simultaneous sparsity selection and positive definite estimation, and BigQUIC in particular is scalable to the ultra high-dimensional  $p = 10^5$  setting considered in this section. Implementations of both these

p	n	CCA		G-IPF		CCA-GIPF		Improvement Factor (G-IPF/CCA Time)
		Time	Norm	Time	Norm	Time	Norm	
500	250	5.2	0.1005	28.6	0.1014	10.1	0.1009	<b>5.5</b>
500	375	5.3	0.0817	28.7	0.0822	10.1	0.0819	<b>5.4</b>
500	500	5.3	0.0700	27.9	0.0703	9.4	0.0701	<b>5.3</b>
500	1000	5.3	0.0492	24.2	0.0493	8.6	0.0493	<b>4.6</b>
1000	500	34.8	0.0762	536.3	0.0765	340.2	0.0762	<b>15.4</b>
1000	750	34.8	0.0626	516.5	0.0627	332.8	0.0625	<b>14.8</b>
1000	1000	34.5	0.0536	513.2	0.0537	333.5	0.0536	<b>14.9</b>
1000	2000	35.3	0.0376	495.1	0.0377	306.8	0.0376	<b>14.0</b>
1500	750	112.7	0.0648	2661.3	0.0643	1885.0	0.0641	<b>23.6</b>
1500	1125	112.9	0.0529	2622.1	0.0525	1841.2	0.0524	<b>23.1</b>
1500	1500	113.0	0.0457	2580.0	0.0453	1809.0	0.0452	<b>22.8</b>
1500	3000	116.0	0.0322	2471.5	0.0318	1737.1	0.0319	<b>21.3</b>
2000	1000	289.8	0.0555	8933.6	0.0551	5179.3	0.0549	<b>30.8</b>
2000	1500	298.9	0.0454	8844.7	0.0450	5112.5	0.0449	<b>29.5</b>
2000	2000	299.5	0.0391	8740.4	0.0387	5016.7	0.0387	<b>29.2</b>
2000	4000	309.3	0.0276	8590.3	0.0273	4870.1	0.0273	<b>27.8</b>
5000	2500	4911.3	0.0320	120252.4	0.0321	33776.3	0.0320	<b>24.5</b>
5000	3750	4945.8	0.0261	113356.6	0.0261	28047.8	0.0261	<b>22.9</b>
5000	5000	5034.5	0.0226	114867.7	0.0226	29037.7	0.0226	<b>22.8</b>
5000	10000	5156.2	0.0160	114133.3	0.0160	29248.7	0.0160	<b>22.1</b>

Table 3: Running time and estimation error (in relative Frobenius norm) for CCA, G-IPF, and CCA-GIPF (use G-IPF with the CCA estimator as the initial value) with normal data. All methods have very similar estimation errors, but CCA is significantly faster. The ratio of running times of G-IPF to CCA is provided in bold.

p	n	CCA		G-IPF		<i>tlasso-IPF</i>		Improvement Factor (G-IPF / CCA Time)
		Time	Norm	Time	Norm	Time	Norm	
500	250	4.0	0.369	54.41	0.372	1933.06	6.862	<b>13.6</b>
500	375	4.0	0.280	36.26	0.282	1792.392	6.817	<b>9.1</b>
500	500	3.9	0.238	37.52	0.239	1772.345	6.779	<b>9.6</b>
500	1000	3.9	0.232	37.27	0.232	1891.426	6.753	<b>9.6</b>
1000	500	27.0	0.322	1548.9	0.323	36508.994	8.878	<b>57.4</b>
1000	750	26.9	0.217	719.9	0.218	35761.71	8.846	<b>26.8</b>
1000	1000	27.9	0.208	650.1	0.208	35364.331	8.838	<b>23.3</b>
1000	2000	28.8	0.170	677.4	0.170	34951.69	8.802	<b>23.5</b>
1500	750	95.193	0.258	6807.133	0.258	185566.52	10.231	<b>71.5</b>
1500	1125	95.517	0.190	3559.467	0.189	185772.6	10.195	<b>37.7</b>
1500	1500	92.459	0.196	3846.347	0.195	180279.2	10.182	<b>41.6</b>
1500	3000	94.754	0.153	3392.462	0.152	174894.6	10.166	<b>35.8</b>
2000	1000	234.100	0.228	12738.264	0.219	> 4 days	NA	<b>54.4</b>
2000	1500	263.570	0.200	17389.751	0.200	> 4 days	NA	<b>66.0</b>
2000	2000	308.789	0.172	10757.530	0.172	> 4 days	NA	<b>34.8</b>
2000	4000	356.389	0.143	11920.13	0.142	> 4 days	NA	<b>33.4</b>
5000	2500	5019.258	0.165	163465.7	0.139	> 4 days	NA	<b>32.6</b>
5000	3750	4817.014	0.118	155700.3	0.118	> 4 days	NA	<b>32.3</b>
5000	5000	5051.542	0.140	159974.9	0.131	> 4 days	NA	<b>31.7</b>
5000	10000	4594.165	0.097	139444.2	0.097	> 4 days	NA	<b>30.4</b>

Table 4: Running time and estimation error (in relative Frobenius norm) for CCA, G-IPF, and *tlasso-IPF* with  $t$  data. G-IPF and CCA again have very similar estimation errors, but CCA is significantly faster. The ratio of running times of G-IPF to CCA is provided in bold, as *tlasso-IPF* values are not available for some of the settings.

RBM	p	n	FST+CCA		Glasso		Improvement Factor $\frac{\text{Glasso}}{\text{FST+CCA}}$
			Time	Norm	Time	Norm	
	1000	500	2.90 secs	0.206	1.44 mins	0.225	<b>29.79</b> times
RBL	p	n	FST+CCA		Glasso		Improvement Factor $\frac{\text{Glasso}}{\text{FST+CCA}}$
			Time	Norm	Time	Norm	
	1000	500	1.25 secs	0.096	2.27 mins	0.241	<b>108.96</b> times
	2000	1000	31.18 secs		0.059	18.19 mins	0.201
							<b>35.00</b> times

Table 5: Running time and estimation error (in relative Frobenius norm) for *FST+CCA* and Glasso, in both RBM and RBL designs, using 1 core. *FST+CCA* is more accurate and significantly faster than Glasso for both designs. The ratio of running times of Glasso to *FST+CCA* is provided in bold.

methods are available in *R*. Simulations comparing the *FST+CCA* method with Glasso consider the setting  $p = \{1000, 2000\}$  with  $n = 0.5p$ , and with BigQUIC use  $p = \{10^4, 10^5\}$ , with  $n = 1000$ . While Glasso is able to comfortably handle settings with a couple of thousand variables, it can be really expensive to allocate enough memory for Glasso to scale to  $p > 10^4$ . Both the dense matrix representations used in the internal steps and the fact that Glasso cannot be straightforwardly parallelized using multiple cores hinder its space and time scalability to ultra-high dimensions. BigQUIC, on the other hand, is able to scale to  $p \gg 10^4$  by employing several innovations which include performing block-wise updates and the use of a fast approximation for the Hessian (see detailed discussion in Hsieh et al. [2013]). As the algorithm is iterative in nature, a ‘bad’ partition of the variables during blocking can hinder its performance. Here we perform the comparative study of the *FST+CCA* method in a single core situation with Glasso when  $p$  is moderately large, and in a multi-core situation with BigQuic with ultra large  $p$ .

For each choice of  $p$ , a true  $\Omega$  is obtained by the random block model (RBM) procedure and also by a random banded line graph (RBL) design procedure, which randomly generates the sub-diagonal entries in the precision matrix that corresponds to a line graph. Both these are described in detail in [Zhang et al., 2021, Section5]. Once this is done, we simulate multivariate Gaussian data with the given true  $\Omega$  as the precision matrix. FST is then applied to this data to determine the graph structure and CCA is applied in parallel to each connected component resulting from FST to obtain the final positive definite estimate of  $\Omega$ . Tuning parameters for FST, Glasso and BigQUIC are determined using five fold cross validation. A total of 50 datasets are generated for each case and the average errors in relative Frobenius norm and average running time are provided in Table 5, 6, and 7.

In Table 5, we provide results for comparison of *FST+CCA* with Glasso in the  $p \in \{1000, 2000\}$  setting. The Glasso implementation available in *R* cannot use parallel processing via multiple cores. While *FST+CCA* has this parallelizable property, for comparison purposes we employ only a single core for all the experiments in Table 5. Even without the benefit of parallel processing, *FST+CCA* is at least 30 to 100 times faster than Glasso, and performs competitively or better than Glasso in terms of accuracy in all settings.

Table 6 provides results for comparing *FST+CCA* with BigQuic in the  $p \in \{1000, 2000\}$  setting, using 16 cores. It shows that *FST+CCA* yields lower wall times and delivers an even better advantage in accuracy. In Table 7, we provide results for comparison of *FST+CCA*

RBM	p	n	FST+CCA		BigQuic		Time Improvement Factor $\frac{\text{BigQuic}}{\text{FST+CCA}}$
			Time	Norm	Time	Norm	
	1000	500	0.77 secs	0.204	1.06 secs	0.286	<b>1.38</b> times
RBL	p	n	FST+CCA		BigQuic		Time Improvement Factor $\frac{\text{BigQuic}}{\text{FST+CCA}}$
			Time	Norm	Time	Norm	
	1000	500	0.43 secs	0.151	1.44 secs	0.303	<b>3.35</b> times
RBL	p	n	FST+CCA		BigQuic		Time Improvement Factor $\frac{\text{BigQuic}}{\text{FST+CCA}}$
			Time	Norm	Time	Norm	
	2000	1000	2.67 secs	0.074	9.46 secs	0.312	<b>3.54</b> times

Table 6: Running time and estimation error (in relative Frobenius norm) for *FST+CCA* and BigQUIC, with  $p = 1000, 2000$ , in both RBM and RBL designs, using 16 cores. *FST+CCA* is more accurate and faster than BigQUIC for both designs. The ratio of running times of BigQUIC to *FST+CCA* is provided in bold.

RBM	p	n	FST+CCA		BigQUIC		Time Improvement Factor (BigQUIC/FST+CCA Time)
			Time	Norm	Time	Norm	
	$10^4$	1000	13.39 secs	0.062	105.13 secs	0.288	<b>7.85</b> times
RBL	p	n	FST+CCA		BigQUIC		Time Improvement Factor (BigQUIC/FST+CCA Time)
			Time	Norm	Time	Norm	
	$10^4$	1000	16.65 secs	0.041	196.45 secs	0.301	<b>11.80</b> times
RBL	p	n	FST+CCA		BigQUIC		Time Improvement Factor (BigQUIC/FST+CCA Time)
			Time	Norm	Time	Norm	
	$10^5$	1000	31.01 mins	0.087	151.70 mins	0.319	<b>4.76</b> times

Table 7: Running time and estimation error (in relative Frobenius norm) for *FST+CCA* and BigQUIC, with  $p = 10^4, 10^5$ , in both RBM and RBL designs, using 16 cores. *FST+CCA* is more accurate and faster than BigQUIC for both designs. The ratio of running times of BigQUIC to *FST+CCA* is provided in bold.

with BigQUIC in the  $p \in \{10^4, 10^5\}$  setting. As mentioned previously, the Glasso implementation in R can break down in these settings due to the use of dense matrix representations. Both *FST+CCA* and BigQUIC however have the ability to use multiple cores for parallel processing, and each method is provided with 16 cores for the experiments in Table 7. In all settings, *FST+CCA* is at least 5 to 12 times faster than BigQUIC, and can also substantially improve accuracy compared to BigQUIC. To summarize, the simulations in this section illustrate that the proposed *FST+CCA* can be significantly faster than state of the art ultra high-dimensional iterative approaches, while providing better estimation accuracy. The results above also underscore how CCA can be readily coupled with high-dimensional sparsity selection methods.

### 5.3 Application to minimum variance portfolio rebalancing

#### 5.3.1 S&P 500 data with 398 stocks when $G$ is given (CCA vs. G-IPF)

The minimum variance portfolio selection problem is defined as follows. Given  $p$  risky assets, let  $r_{ik}$  denote the return of asset  $i$  over time period  $k$  (for  $i = 1, 2, \dots, p$ ); which in turn is defined as the change in its price over time period  $k$ , divided by the price at the beginning of the period. Let  $r_k^T = (r_{1k}, r_{2k}, \dots, r_{pk})$  denote the vector of returns over time period  $k$ . Let

$w_k^T = (w_{1k}, w_{2k}, \dots, w_{pk})$  denote the vector of portfolio weights, i.e.,  $w_{ik}$  denotes the weight of asset  $i$  in the portfolio for the  $k$ -th time period. A long position or a short position for asset  $i$  during period  $k$  is given by the sign of  $w_{ik}$ , i.e.,  $w_{ik} > 0$  for long, and  $w_{ik} < 0$  for short positions respectively. The budget constraint can be written as  $\mathbf{1}^T w_k = 1$ , where  $\mathbf{1}$  denotes the vector of all ones. Let  $\Sigma$  denote the covariance matrix of the vector of returns. Note that the risk of a given portfolio, as measured by the standard deviation of its return, is simply  $(w_k^T \Sigma_k w_k)^{1/2}$ . The minimum variance portfolio selection problem for investment period  $k$  can now be formally defined as follows:  $\min_{w_k} w_k^T \Sigma_k w_k$  subject to  $\mathbf{1}^T w_k = 1$ . As the minimum variance portfolio problem is a simple quadratic program, it has an analytic solution  $w_k^* = (\mathbf{1}^T \Sigma_k^{-1} \mathbf{1})^{-1} \Sigma_k^{-1} \mathbf{1}$ . The most basic approach to the portfolio selection problem often makes the unrealistic assumption that returns are stationary in time. A standard approach to dealing with the non-stationarity in such financial time series is to use a periodic rebalancing strategy. In particular, at the beginning of each investment period  $k = 1, 2, \dots, K$ , portfolio weights  $w_k^T = (w_{1k}, w_{2k}, \dots, w_{pk})$  are computed from the previous  $N_{est}$  days of observed returns ( $N_{est}$  is called the estimation horizon). These portfolio weights are then held constant for the duration of each investment period. The process is repeated at the start of the next investment period and is often referred to as “rebalancing”.

We now consider the problem of investing in the stocks that feature in the S&P 500 index. The S&P 500 is a composite blue chip index consisting of 500 stocks. A number of stocks were removed in our analysis due to limited data span of the corresponding companies as constituents of the S&P 500 index - we ultimately used 398 stocks. For illustration purposes, rebalancing time points were chosen to be every 64 weeks starting from 2000/01/01 to 2016/12/31 (approximately 17 years). Start and end dates of each period are selected to be calendar weeks, and need not coincide with a trading day. The total number of investment periods is 14, and the number of trading days in each investment period is approximately 320 days. We shall compare the performance of two approaches, ones which use G-IPF and CCA for estimating the covariance matrix at each rebalancing point. We consider various choices of  $N_{est}$ , in particular,  $N_{est} \in 375, 450, 525$  in our analysis. Note that once a choice for  $N_{est}$  is made, it is kept constant until the next investment period.

Note that for G-IPF and CCA a graph for the zeros in the concentration matrix is required. When  $N_{est}$  is less than 398, we threshold the generalized inverse for the sample covariance, and when  $N_{est}$  is larger than 398, we threshold the inverse till we achieve a sparsity of approximately 95%. The *Normalized wealth growth* is defined as the accumulated wealth derived from the portfolio over the trading period when the initial budget is normalized to one. This measure is also designed to take into account both transaction costs and borrowing costs. Figure 4 shows that in terms of Normalized Wealth Growth, the G-IPF and CCA based approaches perform very similarly and both perform better than the passive S&P500 index approach (no rebalancing) when  $N_{est} = 375$ . Very similar results are obtained for  $N_{est} = 450$  and 525 (not illustrated here due to space considerations). Overall, the results demonstrate that the CCA and G-IPF based strategies are very competitive with each other in terms of financial performance. However, as demonstrated in Table 8, the CCA algorithm is much faster in terms of computational time compared to the G-IPF approach. Since the inverse covariance matrix has to be estimated at the start of each investment horizon, the gain in computational speed can add up very quickly. The above results reinforce our earlier observations in Section 5.1 that the CCA algorithm provides a significantly more scalable alternative to the G-IPF algorithm, while providing similar statistical performance.

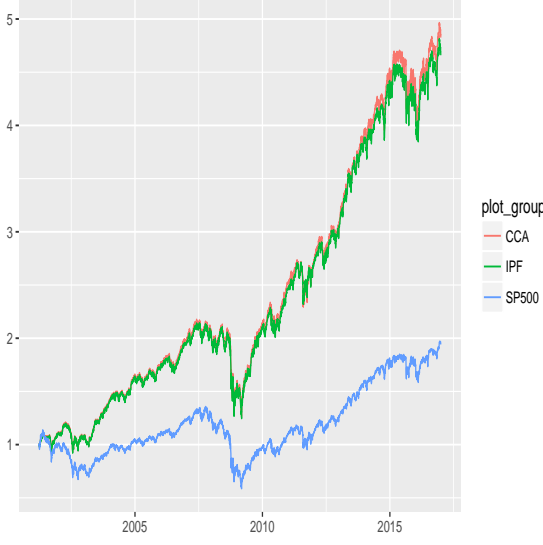


Figure 4: Normalized wealth growth after adjusting for transaction costs (0.5% of principal) and borrowing costs (interest rate of 8% APR) with  $N_{est} = 375$  for S&P 500 data.

	$N_{est}$		
Method	375	450	525
CCA	1.92	1.74	1.67
G-IPF	3.77	4.77	5.31

Table 8: Average running time (in seconds) for estimating the covariance matrix of returns with CCA and G-IPF for various values of  $N_{est}$  for S&P 500 data

### 5.3.2 Kaggle data with 3630 stocks/ETFs when graph $G$ is unknown

In this section, we consider the minimum variance portfolio problem when investing in a much larger number of stocks. The dataset is obtained from an open source publication on Kaggle, provided by Marjanovic [2017]. Specifically 3630 stocks and ETFs which have a complete record from 2014-06-09 to 2017-06-07 (featuring 756 trading days) are selected. Daily returns are calculated. Similar to the previous subsection, we use a rebalancing scheme in this application. A significant difference to address here is that we have fewer number of observations but a much larger number of variables in this dataset. Thus, it is reasonable to choose a relative smaller rebalancing time and larger  $N_{est}$ . We consider the choice of  $N_{est} = 500$ , and rebalancing time of 30 days. This will give us a portfolio to be used from days 501 to 756, which correspond to the period 2016-06-02 to 2017-06-07. More specifically, at beginning, the first 500 daily returns are used to construct a portfolio which will be used in days 501 to 530. Then for days 531 to 560, data from days 31 to 530 will be used for an updated portfolio, and so forth. This scheme gives us a total of 9 time-points for portfolio rebalancing. Here we compare the performance of three approaches, which respectively use *FST+CCA*, Glasso and BigQuic for estimating the precision matrix at each rebalancing point.

For the selection of tuning hyper-parameters, we used the portfolio loss as the loss function and a validation set of size 10. Specifically, for 500 daily return observations, 490 observations were used to construct the portfolio for different tuning parameter values and the last 10 days of portfolio returns were used to determine the best tuning parameter.

The average running time for all the three approaches are recorded in Table 5.3.2. From Table 5.3.2, *FST+CCA* takes about 1/5 of the time required by BigQuic, and less than 1/200 of the time used by Glasso, demonstrating the efficiency of the *FST+CCA* approach.

The normalized wealth growth derived from the portfolios is illustrated in Figure 5, and

Approaches	<i>FST+CCA</i>	BigQuic	Glasso
Running Time (Seconds)	6.883	34.531	1497.781

Table 9: Average running time (in seconds) for estimating the covariance matrix of returns with *FST+CCA*, Glasso and BigQuic, using data on 3630 stocks and ETFs from Marjanovic [2017]

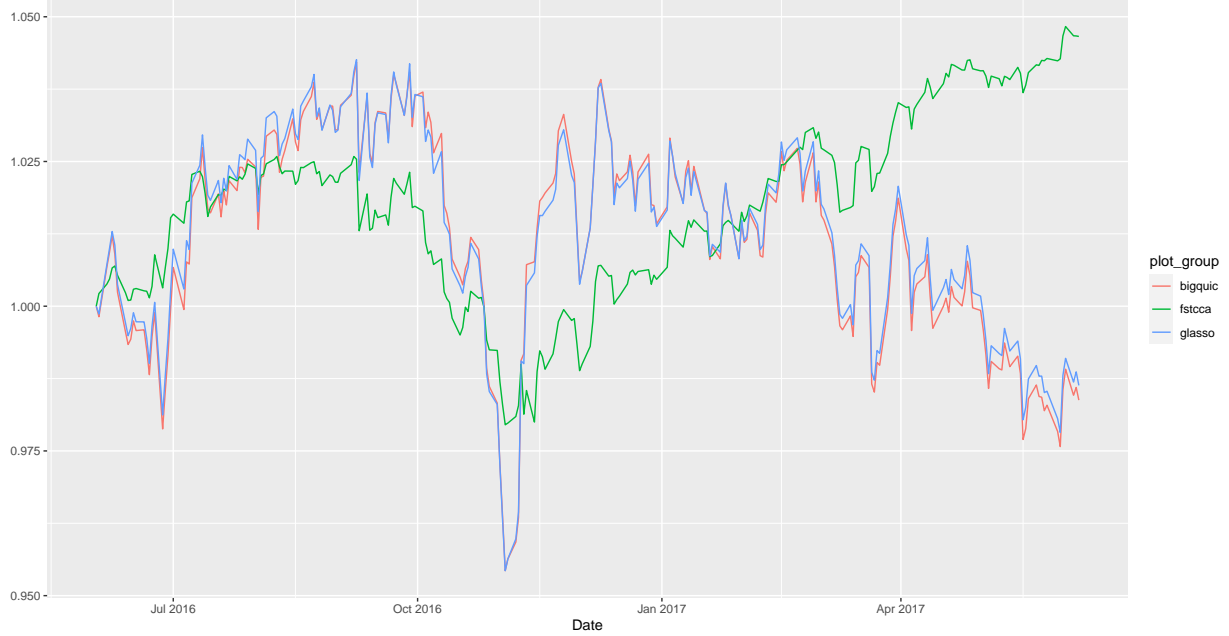


Figure 5: Normalized wealth growth after adjusting for transaction and borrowing costs with  $N_{est} = 500$  for stock/ETF data from Marjanovic [2017].

shows that the *FST+CCA* approach has better overall wealth growth. The daily returns of these portfolios are presented in Figure 6, demonstrating that the *FST+CCA* approach is able to provide a portfolio which is less volatile compared to the other approaches. Overall, *FST+CCA* performs better than the competing methods in terms of both computational efficiency and wealth growth of the associated portfolio.

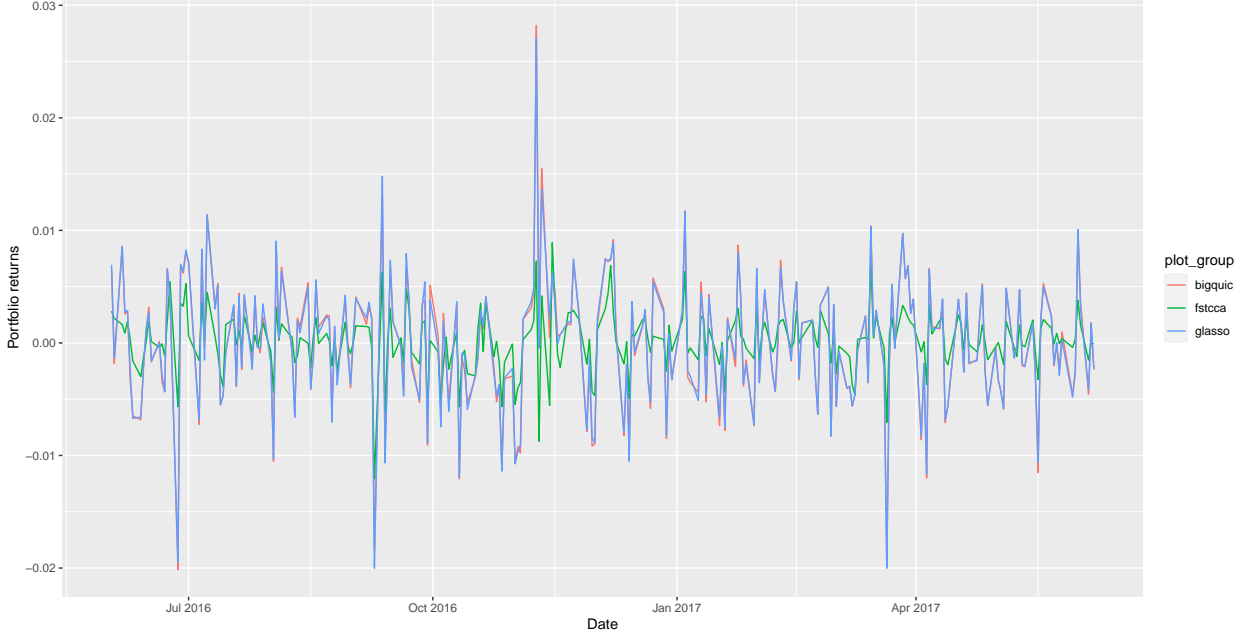


Figure 6: Daily returns corresponding to portfolios associated with various covariance estimation strategies for stock/ETF data from Marjanovic [2017].

## SUPPLEMENTAL MATERIALS

### Section A: Proof of Theorem 1

(a) We first obtain high probability bounds for  $\|\hat{L}^D - \bar{L}\|_2$ . While bounds for  $\|\hat{\Omega}^D - \bar{\Omega}\|_2$  can be obtained by minor changes to the proof of [Rothman et al., 2008, Theorem 1], substantial conceptual and algebraic modifications are needed to derive bounds for  $\|\hat{L}^D - \bar{L}\|_2$ , as presented below.

Let  $\bar{D} = \bar{D}_n$  denote the diagonal matrix whose diagonal entries match those of  $\bar{\Sigma}_n = \bar{\Omega}_n^{-1}$ . Let  $\bar{R} = \bar{R}_n = \bar{D}^{-1/2} \bar{\Sigma}_n \bar{D}^{-1/2}$  denote the population correlation matrix, and let  $\bar{U} = \bar{D}^{1/2} \bar{L}$  denote the Cholesky factor of  $\bar{R}^{-1}$ . At the sample level, let  $\hat{D}$  denote the diagonal matrix whose diagonal entries match those of  $S$ , and  $\hat{R} = \hat{D}^{-1/2} S \hat{D}^{-1/2}$ . Consider the estimator  $\hat{U}^D$  defined by

$$\hat{U}^D = \operatorname{argmin}_{U \in \mathbb{L}_{G^D}} \left\{ \operatorname{tr} \left( U U^T \hat{R} \right) - 2 \log |U| \right\}. \quad (\text{S.1})$$

Using results in Roverato [2002], it follows that

$$\hat{U}_{\cdot j}^{D,>} = - \frac{(\hat{R}^{>j})^{-1} \hat{R}_{\cdot j}^{>}}{\sqrt{\hat{R}_{jj} - (\hat{R}_{\cdot j}^{>})^T (\hat{R}^{>j})^{-1} \hat{R}_{\cdot j}^{>}}} \text{ and } \hat{U}_{jj}^D = \frac{1}{\sqrt{\hat{R}_{jj} - (\hat{R}_{\cdot j}^{>})^T (\hat{R}^{>j})^{-1} \hat{R}_{\cdot j}^{>}}}. \quad (\text{S.2})$$

It follows from Equation (1) of the main paper and (S.2) that  $\hat{L}^D = \hat{D}^{-1/2} \hat{U}^D$ . Using a strategy in Rothman et al. [2008], we will first analyze  $\|\hat{U}^D - \bar{U}\|$ , and leverage this analysis

to bound  $\|\hat{L}^D - \bar{L}\|$ .

Let  $\mathcal{L}_{G_\sigma^D}^*$  denote the space of lower triangular matrices whose  $(i, j)^{th}$  entry is 0 whenever  $(i, j) \notin E_\sigma^D$  (diagonal entries not restricted to be positive). Consider the function

$$\begin{aligned} G(\Delta) &= \text{tr}((\bar{U} + \Delta)(\bar{U} + \Delta)^T \hat{R}) - 2 \log |\bar{U} + \Delta| - \left( \text{tr}((\bar{U} \bar{U}^T \hat{R}) - 2 \log |\bar{U}| \right) \\ &= \text{tr}(\Delta^T \hat{R} \Delta) + 2 \text{tr}(\Delta^T \hat{R} \bar{U}) - 2 \sum_{i=1}^p \log \left( 1 + \frac{\Delta_{ii}}{\bar{U}_{ii}} \right). \end{aligned} \quad (\text{S.3})$$

It is implicitly assumed that  $\Delta_{ii} > -\bar{U}_{ii}$  for every  $1 \leq i \leq p$  so that  $G(\Delta)$  is well-defined. Note that  $G$  is a convex function, and is minimized at  $\hat{\Delta} = \hat{U}^D - \bar{U}$ . Hence,  $G(\hat{\Delta}) \leq 0$ . Let  $\epsilon_n = \sqrt{(|E_\sigma^D| + 1) \log p/n}$ . We will now show that there exists a constant  $M > 0$  such that

$$\inf \left\{ \Delta \in \mathcal{L}_{G_\sigma^D}^* : \|\Delta\|_F = M\epsilon_n \right\} > 0$$

It would then follow that the minimizer  $\hat{\Delta}$  satisfies  $\|\hat{\Delta}\|_2 \leq \|\hat{\Delta}\|_F \leq M\epsilon_n$ . With this goal in mind, fix arbitrarily  $\Delta \in \mathcal{L}_{G_\sigma^D}^*$  such that  $\|\Delta\|_F = M\epsilon_n$ . Using (S.3) and the inequality  $\log(1 + x) \leq x$  for  $x > -1$ , we get

$$\begin{aligned} G(\Delta) &\geq \text{tr}(\Delta^T \hat{R} \Delta) + 2 \text{tr}(\Delta^T \hat{R} \bar{U}) - 2 \sum_{i=1}^p \frac{\Delta_{ii}}{\bar{U}_{ii}} \\ &= \text{tr}(\Delta^T \hat{R} \Delta) + 2 \text{tr}(\Delta^T (\hat{R} - \bar{R}) \bar{U}) + 2 \text{tr}(\Delta^T \bar{R} \bar{U}) - 2 \sum_{i=1}^p \frac{\Delta_{ii}}{\bar{U}_{ii}} \\ &= \text{tr}(\Delta^T \hat{R} \Delta) + 2 \text{tr}((\hat{R} - \bar{R}) \bar{U} \Delta^T) + 2 \text{tr}(\Delta^T (\bar{U}^{-1})^T) - 2 \sum_{i=1}^p \frac{\Delta_{ii}}{\bar{U}_{ii}} \end{aligned} \quad (\text{S.4})$$

Since  $\Delta \in \mathcal{L}_{G_\sigma^D}^*$ , and  $\bar{U}$  is lower triangular, it follows that

$$2 \text{tr}(\Delta^T (\bar{U}^{-1})^T) - 2 \sum_{i=1}^p \frac{\Delta_{ii}}{\bar{U}_{ii}} = 0. \quad (\text{S.5})$$

Also, since  $\sigma$  is a perfect vertex elimination scheme for the decomposable graph  $G_\sigma^D$  and  $\bar{U} \in \mathcal{L}_{G_\sigma^D}$ , it follows that  $(\bar{U} \Delta^T)_{ij} = 0$  if  $(i, j) \notin E_\sigma^D$ . Also, by Assumptions A1 and A2, and [Bickel and Levina, 2008b, Lemma 3], there exists a constant  $\tilde{K}$  such that

$$\max_{1 \leq i, j \leq p} |\hat{R}_{ij} - \bar{R}_{ij}| \leq \tilde{K} \sqrt{\frac{\log p}{n}} \text{ and } \max_{1 \leq i, j \leq p} |S_{ij} - \bar{\Sigma}_{ij}| \leq \tilde{K} \sqrt{\frac{\log p}{n}} \quad (\text{S.6})$$

on an event  $C_n$  where  $P(C_n) \rightarrow 1$  as  $n \rightarrow \infty$ . Since the diagonal entries of  $\hat{R} - \bar{R}$  are zero,

it follows that on  $C_n$

$$\begin{aligned}
|tr\left((\hat{R} - \bar{R})\bar{U}\Delta^T\right)| &= \left| \sum_{(i,j) \in E_\sigma^D} (\hat{R} - \bar{R})_{ij}(\bar{U}\Delta^T)_{ij} \right| \\
&\leq \tilde{K} \sqrt{\frac{\log p}{n}} \sqrt{|E_\sigma^D|} \|\Delta\bar{U}^T\|_F \\
&\leq \frac{\tilde{K}}{\delta} \sqrt{\frac{|E_\sigma^D| \log p}{n}} \|\Delta\|_F \\
&\leq \frac{\tilde{K}}{M\delta} \|\Delta\|_F^2.
\end{aligned} \tag{S.7}$$

Finally, restricting to  $C_n$ , using  $(\Delta\Delta^T)_{ij} = 0$  for  $(i, j) \notin E_\sigma^D$  and Assumption A1, we get

$$\begin{aligned}
tr\left(\Delta^T \hat{R} \Delta\right) &\geq tr\left(\Delta^T \bar{R} \Delta\right) - |tr\left(\Delta^T (\hat{R} - \bar{R}) \Delta\right)| \\
&= tr\left(\Delta^T \bar{R} \Delta\right) - |tr\left(\Delta^T (\hat{R} - \bar{R}) \Delta \Delta^T\right)| \\
&\geq \frac{1}{\delta} \|\Delta\|_F^2 - \left| \sum_{(i,j) \in E_\sigma^D} (\hat{R} - \bar{R})_{ij}(\Delta\Delta^T)_{ij} \right| \\
&\geq \frac{1}{\delta} \|\Delta\|_F^2 - \tilde{K} \sqrt{\frac{\log p}{n}} \sqrt{|E_\sigma^D|} \|\Delta\|_F^2 \\
&\geq \frac{1}{2\delta} \|\Delta\|_F^2
\end{aligned} \tag{S.8}$$

for large enough  $n$ . It follows by (S.4), (S.5), (S.7), (S.8) that  $G(\Delta) > \frac{1}{4\delta} \|\Delta\|_F^2$  for  $M = 8\tilde{K}/\delta$ . Hence

$$P\left(\left\|\hat{U}^D - \bar{U}\right\|_2 \leq \frac{8\tilde{K}}{\delta} \epsilon_n\right) \geq P(C_n) \tag{S.9}$$

for large enough  $n$ . If we restrict to  $C_n$ , it follows from Assumption A1, (S.6) and (S.9) that

$$\begin{aligned}
\left\|\hat{L}^D - \bar{L}\right\|_2 &= \left\|\hat{D}^{-1/2} \hat{U}^D - \bar{D}^{-1/2} \bar{U}\right\|_2 \\
&\leq \|\hat{D}\|_2 \left\|\hat{U}^D - \bar{U}\right\|_2 + \left\|\hat{D}^{-1/2} - \bar{D}^{-1/2}\right\|_2 \|\bar{U}\|_2 \\
&\leq \frac{16\tilde{K}}{\delta^2} \epsilon_n + \frac{2\tilde{K}}{\delta^3} \sqrt{\frac{\log p}{n}} \leq \frac{18\tilde{K}}{\delta^3} \epsilon_n
\end{aligned} \tag{S.10}$$

for large enough  $n$ . The above bound was obtained in terms of  $|E_\sigma^D|$ . Using the closed form representation of  $\hat{L}^D$  in Equation (1) of the main paper, we will now derive another bound for  $\|\hat{L}^D - \bar{L}\|_2$  in terms of  $a^D = a_n^D$ , where  $a_n^D$  is the product of  $\max_{1 \leq j \leq p_n} n_j + 1$  and  $\max_{1 \leq i \leq p_n} r_i + 1$ . Here  $n_j = \{i : 1 \leq j < i \leq p, (i, j) \in E_\sigma^D\}$  and  $r_i = \{j : 1 \leq j < i \leq p, (i, j) \in E_\sigma^D\}$ . For this purpose, we will first bound the  $\ell_2$ -norm of the  $j^{\text{th}}$  column of  $\hat{L}^D - \bar{L}$  for an arbitrary  $1 \leq j \leq p$ . Using Equation (1) of the main paper, Assumption A1,

$\bar{\Omega} \in \mathbb{P}_{G_\sigma^D}$ , and the triangle inequality, we get

$$\|\hat{L}_{.j}^D - \bar{L}_{.j}\|_2 \leq \hat{L}_{jj} \|(S^{>j})^{-1} S_{.j}^> - (\bar{\Sigma}^{>j})^{-1} \bar{\Sigma}_{.j}^>\|_2 + \|(\bar{\Sigma}^{>j})^{-1} \bar{\Sigma}_{.j}^>\|_2 |\hat{L}_{jj} - \bar{L}_{jj}|. \quad (\text{S.11})$$

To bound the above expression, it is key to bound  $\|(S^{>j})^{-1} - (\bar{\Sigma}^{>j})^{-1}\|_2$ . Here  $A^{\geq j} = ((A_{kl}))_{k,l \geq j, (k,j), (l,j) \in E_\sigma^D}$  for any matrix  $A$ . For any  $\mathbf{u} \in \mathbb{R}^{n_j}$  with  $\|\mathbf{u}\|_2 = 1$ , let  $U$  be an  $(n_j + 1) \times (n_j + 1)$  orthogonal matrix with first row  $\mathbf{u}^T$ . Then  $US^{\geq j}U^T$  and  $U\bar{\Sigma}^{\geq j}U^T$  are respectively the sample and population covariance matrix of  $U\mathbf{Y}_1^{\geq j}, U\mathbf{Y}_2^{\geq j}, \dots, U\mathbf{Y}_n^{\geq j}$ . Note that the eigenvalues of  $U\bar{\Sigma}^{\geq j}U^T$  are still uniformly bounded above and below by  $\delta^{-1}$  and  $\delta$  respectively, and  $\mathbf{u}^T S^{\geq j} \mathbf{u}$  is the first diagonal entry of  $US^{\geq j}U^T$  (same with  $\mathbf{u}^T \bar{\Sigma}^{\geq j} \mathbf{u}$ ). It follows by [Bickel and Levina, 2008b, Lemma 3] that

$$P(|\mathbf{u}^T S^{\geq j} \mathbf{u} - \mathbf{u}^T \bar{\Sigma}^{\geq j} \mathbf{u}| \leq \nu) \geq 1 - c_1 \exp(-c_2 n \nu^2) \text{ whenever } |\nu| < \kappa,$$

where  $c_1, c_2, \kappa$  only depend on  $\delta$ . Using the covering arguments in [Vershynin, 2012, Lemma 5.2], it follows that for any constant  $K_1$

$$\begin{aligned} & P \left( \sup_{\|\mathbf{u}\|_2=1} |\mathbf{u}^T S^{\geq j} \mathbf{u} - \mathbf{u}^T \bar{\Sigma}^{\geq j} \mathbf{u}| \leq K_1 \sqrt{\frac{(n_j + 1) \log p}{n}} \right) \\ & \geq 1 - \exp(-K_1^2 (n_j + 1) \log p + 2(n_j + 1) \log 21) \end{aligned}$$

for large enough  $n$ . Since the above holds for every  $1 \leq j \leq p$ , the union-sum inequality can be used to establish the existence of an event  $\tilde{C}_n$  such that  $P(\tilde{C}_n) \rightarrow 1$  as  $n \rightarrow \infty$ , and on the event  $\tilde{C}_n$

$$\|S^{\geq j} - \bar{\Sigma}^{\geq j}\|_2 \leq K_1 \sqrt{\frac{(n_j + 1) \log p}{n}} \quad \forall 1 \leq j \leq p \quad (\text{S.12})$$

for an appropriate constant  $K_1$ . Since  $\max_{1 \leq j \leq p} n_j + 1 = o(n/\log p)$ , it follows from Assumption A1 and (S.12) that on the event  $\tilde{C}_n$

$$\|(S^{>j})^{-1} - (\bar{\Sigma}^{>j})^{-1}\|_2 \leq K_2 \sqrt{\frac{(n_j + 1) \log p}{n}} \quad \forall 1 \leq j \leq p \quad (\text{S.13})$$

for an appropriate constant  $K_2$ . Using (S.13) along with the fact that the first diagonal entries of  $(S^{>j})^{-1}$  and  $(\bar{\Sigma}^{>j})^{-1}$  are  $\hat{L}_{jj}^2$  and  $\bar{L}_{jj}^2$  respectively, we get

$$|\hat{L}_{jj}^2 - \bar{L}_{jj}^2| \leq K_2 \sqrt{\frac{(n_j + 1) \log p}{n}}$$

for  $1 \leq j \leq p$  on  $\tilde{C}_n$ . Using Assumption A1 along with  $|\hat{L}_{jj} - \bar{L}_{jj}| = |\hat{L}_{jj}^2 - \bar{L}_{jj}^2|/|\hat{L}_{jj} + \bar{L}_{jj}|$ , we get

$$|\hat{L}_{jj} - \bar{L}_{jj}| \leq \frac{K_2}{\delta} \sqrt{\frac{(n_j + 1) \log p}{n}} \quad (\text{S.14})$$

Since  $\hat{L}_{ii}^2 (S^{>j})^{-1} S_{.j}^>$  is the first column of  $(S^{>j})^{-1}$  (sans the diagonal entry), and  $\bar{L}_{ii}^2 (\bar{\Sigma}^{>j})^{-1} \bar{\Sigma}_{.j}^>$

is the first column of  $(\bar{\Sigma}^{\geq j})^{-1}$ , it follows from (S.11), (S.13) and (S.14) that

$$\|\hat{L}_{\cdot j}^D - \bar{L}_j\|_2 \leq K_3 \sqrt{\frac{(n_j + 1) \log p}{n}} \quad (\text{S.15})$$

for every  $1 \leq j \leq p$  on  $\tilde{C}_n$ . For any  $\mathbf{v} \in \mathbb{R}^p$  with  $\|\mathbf{v}\|_2 = 1$ , we get by (S.15) and the Cauchy-Schwarz inequality that

$$\begin{aligned} \|(\hat{L}^D - \bar{L})\mathbf{v}\|_2^2 &= \sum_{i=1}^p \left( \sum_{j \leq i: i=j \text{ or } (i,j) \in E_\sigma^D} (\hat{L}^D - \bar{L})_{ij} v_j \right)^2 \\ &\leq \sum_{i=1}^p (r_i + 1) \sum_{j \leq i: i=j \text{ or } (i,j) \in E_\sigma^D} (\hat{L}^D - \bar{L})_{ij}^2 v_j^2 \\ &\leq \left( \max_{1 \leq i \leq p} r_i + 1 \right) \sum_{j=1}^p v_j^2 \left( \sum_{i \geq j: i=j \text{ or } (i,j) \in E_\sigma^D} (\hat{L}^D - \bar{L})_{ij}^2 \right) \\ &= \left( \max_{1 \leq i \leq p} r_i + 1 \right) \sum_{j=1}^p v_j^2 \|\hat{L}_{\cdot j}^D - \bar{L}_j\|_2^2 \\ &\leq K_3^2 \frac{a_n^D \log p}{n} \|\mathbf{v}\|_2^2 \end{aligned}$$

on  $\tilde{C}_n$ . It follows by the above inequality and (S.10) that

$$\|\hat{L}^D - \bar{L}\|_2 \leq \max \left( K_3, \frac{18\tilde{K}}{\delta^3} \right) \sqrt{\frac{\min(a_n^D, |E_\sigma^D| + 1) \log p}{n}} \quad (\text{S.16})$$

on  $C_n \cap \tilde{C}_n$ . Note that  $P(C_n \cap \tilde{C}_n) \rightarrow 1$  as  $n \rightarrow \infty$ . This establishes part (a).

(b) Let  $c = |E_\sigma^D \setminus E_\sigma|$ . In other words,  $c$  is the number of fill-in entries. Consider row-wise traversal of a lower triangular matrix as described in Step II of the CCA algorithm: start with the second row and move from entries with the lowest column index to the highest column index before the diagonal. We order the fill-in entries based on when they are encountered in this traversal. We define functions  $\mathcal{U}$  and  $\mathcal{V}$  from  $\{1, 2, \dots, c\}$  to  $\{1, 2, \dots, p\}$  such that  $(\mathcal{U}(r), \mathcal{V}(r))$  is the  $r^{th}$  fill-in entry, for  $1 \leq r \leq c$ . For  $0 \leq r \leq c$ , let  $\hat{L}^{(r)}$  denote the intermediate matrix which is obtained by updating the first  $r$  fill in entries as in in Algorithm 1 of the main paper, and  $\hat{\Omega}^{(r)} = \hat{L}^{(r)}(\hat{L}^{(r)})^T$ . In particular,  $\hat{L}^{(0)} = \hat{L}^D$  while  $\hat{L}^{(c)} = \hat{L}$  (the CCA estimator).

Henceforth, we will restrict to the event  $C_n \cap \tilde{C}_n$ . Let

$$\tilde{\epsilon}_n = \max(K_3, 18\tilde{K}\delta^{-3}) \sqrt{\frac{\min(a_n^D, |E_\sigma^D| + 1) \log p}{n}},$$

and let  $N \in \mathbb{N}$  be such that  $\tilde{\epsilon}_n (1 + \max_{1 \leq r \leq c} g^D(r)) < \frac{\sqrt{\delta}}{2}$  for  $n > N$ . Note that the matrices

$\hat{L}^{(1)}$  and  $\hat{L}^{(0)}$  only differ in the  $(\mathcal{U}(1), \mathcal{V}(1))^{th}$  entry. Hence

$$\begin{aligned}
\left\| L^{(\hat{1})} - \bar{L} \right\|_2 &\leq \left\| L^{(1)} - L^{(0)} \right\|_2 + \left\| L^{(0)} - \bar{L} \right\|_2 \\
&= \left| \hat{L}_{\mathcal{U}(1), \mathcal{V}(1)}^{(1)} - \hat{L}_{\mathcal{U}(1), \mathcal{V}(1)}^{(0)} \right| + \left\| L^{(0)} - \bar{L} \right\|_2 \\
&= \left| \hat{L}_{\mathcal{U}(1), \mathcal{V}(1)}^{(0)} + \frac{\sum_{k < \mathcal{V}(1)} \hat{L}_{\mathcal{U}(1), k}^{(0)} \hat{L}_{\mathcal{V}(1), k}^{(0)}}{\hat{L}_{\mathcal{V}(1), \mathcal{V}(1)}^{(0)}} \right| + \left\| \hat{L}^{(0)} - \bar{L} \right\|_2 \\
&\leq \frac{\left| \hat{\Omega}_{\mathcal{U}(1), \mathcal{V}(1)}^{(0)} \right|}{\left| \hat{L}_{\mathcal{V}(1), \mathcal{V}(1)}^{(0)} \right|} + \left\| \hat{L}^{(0)} - \bar{L} \right\|_2 \\
&= \frac{\left| \hat{\Omega}_{\mathcal{U}(1), \mathcal{V}(1)}^{(0)} - \bar{\Omega}_{\mathcal{U}(1), \mathcal{V}(1)} \right|}{\left| \hat{L}_{\mathcal{V}(1), \mathcal{V}(1)}^{(0)} \right|} + \left\| \hat{L}^{(0)} - \bar{L} \right\|_2
\end{aligned}$$

Note that  $\left\| \bar{\Omega} \right\|_2 = \left\| \bar{L} \bar{L}^T \right\|_2 = \left\| \bar{L} \right\|_2^2 \leq \frac{1}{\delta}$ . It follows that

$$\begin{aligned}
\left\| \hat{\Omega}^{(0)} - \bar{\Omega} \right\|_2 &= \left\| \hat{L}^{(0)} (\hat{L}^{(0)})^T - \bar{L} \bar{L}^T \right\|_2 \\
&\leq \left\| \hat{L}^{(0)} \right\|_2 \left\| \hat{L}^{(0)} - \bar{L} \right\|_2 + \left\| \bar{L} \right\|_2 \left\| \hat{L}^{(0)} - \bar{L} \right\|_2 \\
&= (\left\| \hat{L}^{(0)} \right\|_2 + \left\| \bar{L} \right\|_2) \left\| \hat{L}^{(0)} - \bar{L} \right\|_2 \\
&\leq (\left\| \hat{L}^{(0)} - \bar{L} \right\| + 2 \left\| \bar{L} \right\|_2) \left\| \hat{L}^{(0)} - \bar{L} \right\|_2 \\
&\leq \frac{3}{\sqrt{\delta}} \left\| \hat{L}^{(0)} - \bar{L} \right\|_2
\end{aligned}$$

on  $C_n \cap \tilde{C}_n$  for large enough  $n$ . The last inequality follows from (S.16) and  $\sqrt{\frac{\min(a_n^D, |E_\sigma^D|+1) \log p}{n}} = o(1)$ . Also by (S.16), as  $\bar{L}_{ii} \geq \sqrt{\delta}$  and  $\left| \hat{L}_{ii}^{(0)} \right| \geq \left| \bar{L}_{ii} \right| - \left| \bar{L}_{ii} - \hat{L}_{ii}^{(0)} \right|$ , we have  $\left| \hat{L}_{ii}^{(0)} \right| \geq \frac{\sqrt{\delta}}{2}$  for every  $1 \leq i \leq p$  on  $C_n \cap \tilde{C}_n$  for large enough  $n$ . It follows that,

$$\left| \hat{L}_{\mathcal{U}(1), \mathcal{V}(1)}^{(1)} - \hat{L}_{\mathcal{U}(1), \mathcal{V}(1)}^{(0)} \right| \leq \frac{6}{\delta} \tilde{\epsilon}_n = g^D(1) \quad (\text{S.17})$$

for  $n > N$ . We will now proceed by induction. Suppose

$$\left| \hat{L}_{\mathcal{U}(\tilde{r}), \mathcal{V}(\tilde{r})}^{(\tilde{r})} - \hat{L}_{\mathcal{U}(\tilde{r}), \mathcal{V}(\tilde{r})}^{(0)} \right| \leq g^D(\tilde{r}) \tilde{\epsilon}_n$$

for  $1 \leq \tilde{r} \leq r-1$ . Note that

$$\left| \hat{L}_{\mathcal{U}(r), \mathcal{V}(r)}^{(r)} - \hat{L}_{\mathcal{U}(r), \mathcal{V}(r)}^{(0)} \right| = \left| \hat{L}_{\mathcal{U}(r), \mathcal{V}(r)}^{(0)} + \frac{\sum_{k < \mathcal{V}(r)} \hat{L}_{\mathcal{U}(r), k}^{(r-1)} \hat{L}_{\mathcal{V}(r), k}^{(r-1)}}{\hat{L}_{\mathcal{V}(r), \mathcal{V}(r)}^{(0)}} \right|.$$

Note that the entries of  $\hat{L}^{(r-1)}$  and  $\hat{L}^{(0)}$  match except for the first  $r-1$  fill-in entries. Recall that  $\tilde{r} \in \mathcal{F}_r^D$  if and only if  $(\mathcal{U}(\tilde{r}), \mathcal{V}(\tilde{r})) = (\mathcal{U}(r), k)$  and  $((\mathcal{V}(r), k) \in E_\sigma^D$  for some  $k < \mathcal{V}(r)$  or

$(\mathcal{U}(\tilde{r}), \mathcal{V}(\tilde{r})) = (\mathcal{V}(r), k)$  and  $(\mathcal{U}(r), k) \in E_\sigma^D$  for some  $k < \mathcal{V}(r)$ . By the induction hypothesis, (S.16), and the choice of  $N$ , it follows that  $|\hat{L}_{ij}^{(\tilde{r})}| \leq \frac{3}{2\sqrt{\delta}}$  whenever  $i > j$ , and  $|\hat{L}_{ij}^{(\tilde{r})}| \geq \frac{\sqrt{\delta}}{2}$  whenever  $i = j$ . Using  $|ab - a_0b_0| \leq |a||b - b_0| + |b_0||a - a_0|$  (in case there is a  $k < \mathcal{V}(r)$  such that  $(\mathcal{U}(r), k)$  and  $(\mathcal{V}(r), k)$  are both fill-in entries) along with the above observations we get

$$\begin{aligned}
& \left| \hat{L}_{\mathcal{U}(r), \mathcal{V}(r)}^{(r)} - \hat{L}_{\mathcal{U}(r), \mathcal{V}(r)}^{(0)} \right| \\
& \leq \left| \hat{L}_{\mathcal{U}(r), \mathcal{V}(r)}^{(0)} + \frac{\sum_{k < \mathcal{V}(r)} \hat{L}_{\mathcal{U}(r), k}^{(0)} \hat{L}_{\mathcal{V}(r), k}^{(0)}}{\hat{L}_{\mathcal{V}(r), \mathcal{V}(r)}^{(0)}} \right| + \frac{3}{\delta} \sum_{\tilde{r} \in \mathcal{F}_r^D} \left| \hat{L}_{\mathcal{U}(\tilde{r}), \mathcal{V}(\tilde{r})}^{(\tilde{r})} - \hat{L}_{\mathcal{U}(\tilde{r}), \mathcal{V}(\tilde{r})}^{(0)} \right| \\
& \leq \frac{\left| \hat{\Omega}_{\mathcal{U}(r), \mathcal{V}(r)}^{(0)} - \bar{\Omega}_{\mathcal{U}(r), \mathcal{V}(r)} \right|}{\left| \hat{L}_{\mathcal{V}(r), \mathcal{V}(r)}^{(0)} \right|} + \frac{3}{\delta} \sum_{\tilde{r} \in \mathcal{F}_r^D} g^D(\tilde{r}) \tilde{\epsilon}_n \\
& \leq \frac{3}{\delta} \left( 2 + \sum_{\tilde{r} \in \mathcal{F}_r^D} g^D(\tilde{r}) \right) \tilde{\epsilon}_n = g^D(r) \tilde{\epsilon}_n.
\end{aligned}$$

By induction, it follows that

$$\left| \hat{L}_{\mathcal{U}(r), \mathcal{V}(r)}^{(r)} - \hat{L}_{\mathcal{U}(r), \mathcal{V}(r)}^{(0)} \right| \leq g^D(r) \tilde{\epsilon}_n \quad \forall 1 \leq r \leq c.$$

This implies

$$\left\| \hat{L} - \bar{L}^D \right\|_{max} = \left\| \hat{L}^{(c)} - \hat{L}^{(0)} \right\|_{max} \leq \tilde{\epsilon}_n \max_{1 \leq r \leq c} g^D(r),$$

Using a similar argument as the one right before (S.16), we get

$$\left\| \hat{L} - \hat{L}^D \right\|_2 \leq \tilde{\epsilon}_n \sqrt{\tilde{a}_n^D} \max_{1 \leq r \leq c} g^D(r)$$

where  $\tilde{a}_n^D$  is the product of the maximum number of fill-in entries in any given column and the maximum number of fill-in entries in any given row. It follows that on  $C_n \cap \tilde{C}_n$

$$\left\| \hat{L} - \bar{L} \right\|_2 \leq \tilde{\epsilon}_n \left( \sqrt{\tilde{a}_n^D} \max_{1 \leq r \leq c} g^D(r) + 1 \right) \leq K \sqrt{\frac{s_{CCA} \log p}{n}} \quad (\text{S.18})$$

for an appropriate constant  $K$ . Finally, note that

$$\begin{aligned}
\left\| \hat{\Omega} - \bar{\Omega} \right\|_2 &= \left\| \hat{L} \hat{L}^T - \bar{L} \bar{L}^T \right\|_2 \\
&= \left\| \hat{L} \hat{L}^T - \bar{L} \hat{L}^T + \bar{L} \hat{L}^T - \bar{L} \bar{L}^T \right\|_2 \\
&\leq \left\| \hat{L} - \bar{L} \right\|_2 \left\| \hat{L} \right\|_2 + \left\| \bar{L} \right\|_2 \left\| \hat{L} - \bar{L} \right\|_2 \\
&\leq \left\| \hat{L} - \bar{L} \right\|_2^2 + 2 \left\| \bar{L} \right\|_2 \left\| \hat{L} - \bar{L} \right\|_2 \\
&\leq K' \sqrt{\frac{s_{CCA} \log p}{n}}
\end{aligned}$$

on  $C_n \cap \tilde{C}_n$  for an appropriate constant  $K'$ . The last inequality follows from (S.18), Assumption A1 and Assumption A2.  $\square$

## Section B: Weak convergence with fixed $p$

We start by establishing two lemmas which imply that  $\hat{\Omega}$  is a differentiable function of  $\Omega$ .

**Lemma S.1** *The function  $\phi_{1,G_\sigma^D} : \mathbb{P}^+ \rightarrow \mathbb{P}_{G_\sigma^D}$  defined by*

$$\phi_{1,G_\sigma^D}(A) = \sum_{C \in \mathbb{C}_\sigma^D} [(A^{-1})_C]^0 - \sum_{Sep \in \mathcal{S}_\sigma^D} [(A^{-1})_{Sep}]^0$$

*is differentiable. Also, if  $A^{-1} \in \mathbb{P}_{G_\sigma^D}$ , then  $\phi_{1,G_\sigma^D}(A) = A^{-1}$ .*

*Proof:* The differentiability follows by repeated application of the differentiability of the matrix inverse for positive definite matrices. It is known that (see Lauritzen [1996])  $\phi_{1,G_\sigma^D}(A)$  uniquely minimizes the function

$$f(K) = \text{tr}(KA) - |KA|$$

for  $K \in \mathbb{P}_{G_\sigma^D}$ . Since  $A^{-1}$  uniquely minimizes  $f$  over the space of all positive definite matrices, if  $A^{-1} \in \mathbb{P}_{G_\sigma^D}$ , it follows that  $\phi_{1,G_\sigma^D}(A) = A^{-1}$ .  $\square$

Let  $\phi_{2,G_\sigma} : \mathbb{L}^+ \rightarrow \mathbb{L}_{G_\sigma}$  be defined as the function which takes  $L \in \mathbb{L}^+$ , and applies the last step of Algorithm 1 of the main paper (with the two *for* loops) to convert it to a matrix in  $\mathcal{L}_{G_\sigma}$ .

**Lemma S.2** *The function  $\phi_{3,G_\sigma} : \mathbb{P}^+ \rightarrow \mathbb{P}_{G_\sigma}$  defined by*

$$\phi_{3,G_\sigma}(A) = \phi_{2,G_\sigma}(L_A) \phi_{2,G_\sigma}(L_A)^T$$

*is differentiable. Here  $L_A$  denotes the Cholesky factor of  $A$ . Also, if  $A \in \mathbb{P}_{G_\sigma}$ , then  $\phi_{3,G_\sigma}(A) = A$ .*

*Proof:* The transformation of a positive definite matrix  $A$  to its Cholesky factor  $L_A$  is clearly differentiable. It is clear from construction that for  $i > j$ ,  $(\phi_{2,G_\sigma}(L_A))_{ij}$  is a polynomial in  $((L_A)_{ij}, \{\phi_{2,G_\sigma}(L_A)_{ik}\}_{k < j}, \{\phi_{2,G_\sigma}(L_A)_{jk}\}_{k < j}, \frac{1}{(L_A)_{jj}})$ . Since all the diagonal entries of  $\phi_{2,G_\sigma}(L_A)$  are the same as the diagonal entries of  $L_A$ , it follows that the entries of  $\phi_{2,G_\sigma}(L_A)$  are polynomials in entries of  $L_A$  and  $\left\{ \frac{1}{(L_A)_{ii}} \right\}_{1 \leq i \leq p}$ , which implies that all the entries of  $\phi_{3,G_\sigma}(A)$  are polynomials in the entries of  $L_A$  and  $\left\{ \frac{1}{(L_A)_{ii}} \right\}_{1 \leq i \leq p}$ . Hence,  $\phi_{3,G_\sigma}$  is a differentiable transformation from  $\mathbb{P}^+$  to  $\mathbb{P}_{G_\sigma}$ .

Suppose  $A \in \mathbb{P}_{G_\sigma}$ . It follows that  $L_A \in \mathcal{L}_{G_\sigma}$ . We prove by induction that  $\phi_{2,G_\sigma}$  does not alter  $L_A$ . This would clearly imply  $\phi_{3,G_\sigma}(A) = A$ . Note that all the diagonal entries of  $L_A$  are not altered by  $\phi_{2,G_\sigma}$ . Suppose that all the entries of  $\phi_{2,G_\sigma}(L_A)$  and  $L_A$  are the same for the first  $i-1$  rows, and the first  $j-1$  entries of the  $i^{\text{th}}$  row, for some  $i > j$ . If  $(i, j) \in E_\sigma$ , then by construction  $\phi_{2,G_\sigma}(L_A)_{ij} = (L_A)_{ij}$ . If  $(i, j) \notin E_\sigma$ , then by the induction hypothesis

and the fact that  $L_A \in \mathcal{L}_{G_\sigma}$ , it follows that

$$\begin{aligned}\phi_{2,G_\sigma}(L_A)_{ij} &= \frac{-\sum_{k=1}^{j-1} \phi_{2,G_\sigma}(L_A)_{ik} \phi_{2,G_\sigma}(L_A)_{jk}}{\phi_{2,G_\sigma}(L_A)_{jj}} \\ &= \frac{-\sum_{k=1}^{j-1} (L_A)_{ik} (L_A)_{jk}}{(L_A)_{jj}} \\ &= (L_A)_{ij}.\end{aligned}$$

The result follows by induction.  $\square$

Using the above lemmas, we now establish weak convergence of the estimator corresponding to Algorithm 1 of the main paper.

**Theorem S.1** *Under the assumption in Equation 5 of the main paper, the estimator  $\widehat{\Omega}$  obtained from Algorithm 1 of the main paper is  $\sqrt{n}$ -consistent. In particular,  $\sqrt{n}(\widehat{\Omega} - \bar{\Omega})$  converges to a multivariate Gaussian limit as  $n \rightarrow \infty$ .*

*Proof:* Note that  $\widehat{\Omega}^D = \phi_{1,G_\sigma}(S)$  and  $\widehat{\Omega} = \phi_{3,G_\sigma}(\widehat{\Omega}^D)$ . Hence, we get that  $\widehat{\Omega} = \phi_{3,G_\sigma}(\phi_{1,G_\sigma}(S))$ . Since  $\bar{\Omega} \in \mathbb{P}_{G_\sigma}$ , it follows that  $\bar{\Omega} = \phi_{3,G_\sigma}(\phi_{1,G_\sigma}(\bar{\Omega}))$ . Using the multivariate Delta method along with these observations establishes the convergence of  $\sqrt{n}(\widehat{\Omega} - \bar{\Omega})$  to a multivariate Gaussian limit as  $n \rightarrow \infty$ .  $\square$

## Section C: Proof of Lemma 1

Note that the assumption that  $n$  is greater than the largest clique size in  $G_\sigma^D$  is required for the existence of  $\widehat{\Omega}^D$ , which in turn is needed for Algorithm 1 in the main paper. Let  $\widehat{L}$  denote the Cholesky factor of  $\widehat{\Omega}$ . It is clear by construction that  $\widehat{L} \in \mathbb{L}_{G_\sigma^D}$ , and  $\widehat{\Omega} \in \mathbb{P}_{G_\sigma^D}$ . Note that if  $i > j$ ,  $(i, j) \notin E_\sigma^D \setminus E_\sigma$ , then  $\widehat{L}_{ij} = -\sum_{k=1}^{j-1} \widehat{L}_{ik} \widehat{L}_{jk} / \widehat{L}_{jj}$ . Hence

$$\widehat{\Omega}_{ij} = (\widehat{L} \widehat{L}^T)_{ij} = \sum_{k=1}^j \widehat{L}_{ik} \widehat{L}_{jk} = \widehat{L}_{ij} \widehat{L}_{jj} + \sum_{k=1}^{j-1} \widehat{L}_{ik} \widehat{L}_{jk} = 0.$$

It follows that  $\widehat{L} \in \mathbb{L}_{G_\sigma}$  and  $\widehat{\Omega} \in \mathbb{P}_{G_\sigma}$ .  $\square$

## Section D: Proof of Lemma 2

The fact that  $\widehat{L}$  is a minimizer of  $h(\cdot)$  over the relevant set follows from the fact that  $h$  is non-negative,  $h(\widehat{L}) = 0$ , and Lemma 1 in the main paper. Suppose  $\tilde{L}$  is another minimizer of  $h$  over the relevant set. Then  $h(\tilde{L}) = 0$ , which implies that  $\tilde{L}_{ij} = \widehat{L}_{ij}^D = \widehat{L}_{ij}$  if  $(i, j) \in E_\sigma$  or  $i = j$ . Suppose there are  $c$  fill-in entries for  $\widehat{L}^D$  with row-column locations given by  $(i_1, j_1), (i_2, j_2), \dots, (i_c, j_c)$ . The entries are ordered based on the traversal of  $\widehat{L}^D$  described in Step II above. Since  $(\tilde{L} \tilde{L}^T)_{i_1 j_1} = 0$ , it follows that

$$\tilde{L}_{i_1 j_1} = -\frac{\sum_{k=1}^{j_1-1} \tilde{L}_{i_1 k} \tilde{L}_{j_1 k}}{\tilde{L}_{j_1 j_1}}.$$

Since all entries on the RHS are not fill-in entries and  $\widehat{\Omega}_{i_1 j_1} = (\widehat{L} \widehat{L}^T)_{i_1 j_1} = 0$ , it follows that  $\tilde{L}_{i_1 j_1} = \widehat{L}_{i_1 j_1}$ . Similarly, if  $c \geq 2$ , note that

$$\tilde{L}_{i_r j_r} = -\frac{\sum_{k=1}^{j_r-1} \tilde{L}_{i_r k} \tilde{L}_{j_r k}}{\tilde{L}_{j_r j_r}}$$

for every  $2 \leq r \leq c$ . The entries on the RHS are either non fill-in entries or among the first  $r-1$  fill-in entries. Hence, by a straightforward induction argument it follows that  $\tilde{L}$  and  $\widehat{L}$  share values even at the fill-in locations.  $\square$

## Section E: Proof of Lemma 5

First let us assume  $G$  is connected. Then

$$2p^2|E_\sigma| = p^2 \sum_{i=1}^p |\{j : (i, j) \in E_\sigma\}| \geq p^2 \times p = p^3.$$

Similarly

$$p^2 \sum_{U \in \mathcal{U}} |U| = p^2 \sum_{U \in \mathcal{U}} \sum_{i \in U} 1 = p^2 \sum_{i \in V} \sum_{U \in \mathcal{U}: i \in U} 1 \geq p^2 \sum_{i \in V} 1 = p^3.$$

The result now follows by Table 1 in the main paper. For disconnected graphs, the inequalities above hold for each respective connected component. Since the overall complexity for all algorithms is obtained by adding the complexities over all connected components, the result follows for disconnected graphs as well.  $\square$

## Section F: Proof of Lemma 6

Let  $c_p = \binom{p}{2}$  and  $d_p = p^{5/3}$  for convenience. Then

$$|\mathcal{A}_p| = 2^{c_p} - |\mathcal{A}_p^c| = 2^{c_p} - \sum_{k=0}^{d_p} \binom{c_p}{k} \geq 2^{c_p} - (d_p + 1) \binom{c_p}{d_p}$$

for  $p \geq 100$ , since  $\binom{n}{r}$  increases in  $r$  for  $r < n/2$  and  $d_p < c_p/2$  for  $p \geq 100$ . Using Stirling's approximation, it follows that

$$|\mathcal{A}_p| \geq 2^{c_p} - (d_p + 1) \frac{c_p^{d_p}}{d_p!} \geq 2^{c_p} - C \sqrt{d_p} \left( \frac{ec_p}{d_p} \right)^{d_p} \geq 2^{c_p} - C \sqrt{d_p} (ec_p)^{d_p}$$

where  $C = \sqrt{2/\pi}$ . Since  $p^2/4 \leq c_p \leq p^2/2$  for  $p \geq 100$ , it follows that

$$\frac{|\mathcal{A}_p|}{2^{c_p}} \geq 1 - C \exp \left( \frac{5}{6} \log p + d_p + 2d_p \log p - c_p \log 2 \right) \geq 1 - C \exp \left( 3d_p \log p - \frac{p^2 \log 2}{4} \right) \rightarrow 1$$

as  $p \rightarrow \infty$ . This establishes part (a). For part (b), note that for any ordering  $\sigma$  of the  $p$

vertices,  $|E_\sigma^D| \geq |E_\sigma| > p^{5/3}$ . Hence, the CCA algorithm uses a direct computation of  $\hat{L}^D$  (see equation (3) in the main paper) and has computational complexity  $O(p^3)$ . On the other hand, it can be seen using Jensen's inequality (similar to equation (3) in the main paper) that

$$\sum_{j=1}^p \tilde{n}_j^3 \geq p \left( \frac{1}{p} \sum_{j=1}^p \tilde{n}_j \right)^3 = \frac{|E_\sigma|^3}{p^2} \geq p^3.$$

□

## Section G: Proof of Lemma 7

Since  $\hat{\Omega}_{32} = 0$ , it follows that

$$\hat{L}_{32} = -\frac{\hat{L}_{21}\hat{L}_{31}}{\hat{L}_{22}}.$$

Next, using  $\hat{\Omega}_{43} = 0$  along with the above equality, it follows that

$$\hat{L}_{43} = -\frac{\hat{L}_{42}\hat{L}_{32}}{\hat{L}_{33}} = \frac{\hat{L}_{21}\hat{L}_{31}\hat{L}_{42}}{\hat{L}_{22}\hat{L}_{33}}.$$

Sequentially extending these calculations to include all fill-in entries, we obtain

$$\hat{L}_{i,i-1} = (-1)^{i-2} \hat{L}_{i,i-2} \frac{\hat{L}_{21}}{\hat{L}_{22}} \prod_{j=3}^{i-1} \frac{\hat{L}_{j,j-2}}{\hat{L}_{jj}} \quad (\text{S.19})$$

for  $4 \leq i \leq p-1$ . Since  $\Omega_0 \in \mathbb{P}_{G_\sigma}$ , identical calculations lead to

$$\bar{L}_{32} = -\frac{\bar{L}_{21}\bar{L}_{31}}{\bar{L}_{22}} \text{ and } \bar{L}_{i,i-1} = (-1)^{i-2} \bar{L}_{i,i-2} \frac{\bar{L}_{21}}{\bar{L}_{22}} \prod_{j=3}^{i-1} \frac{\bar{L}_{j,j-2}}{\bar{L}_{jj}} \quad (\text{S.20})$$

for  $4 \leq i \leq p-1$ . In (S.19) and (S.20), all fill-in entries of the respective Cholesky matrices are expressed in terms of the non fill-in entries of these matrices. Note that  $a_n^D = O(1)$  in this setting. By repeating the arguments in the proof of part (a) of Theorem 1 after equation (S.10), there exists an appropriate positive constant  $K^*$  such that

$$\|\hat{L}^D - \bar{L}\|_2 \leq \tilde{K}^* \sqrt{\frac{\log p}{n}}$$

on an event  $\tilde{D}_n$  with  $\bar{P}(\tilde{D}_n) \rightarrow 1$  as  $n \rightarrow \infty$ . Let  $\tilde{\delta} > 0$  be such that

$$\frac{2\tilde{\delta}}{\delta} + \frac{4\tilde{\delta}}{\delta^3} < \frac{1-\xi}{2}, \quad (\text{S.21})$$

where  $\xi := \sup_{n \geq 1} \max_{3 \leq j \leq p-1} \frac{|\bar{L}_{j,j-2}|}{\bar{L}_{jj}} < 1$  by Assumption A3'. Since  $\hat{L}_{i,j}^D = \hat{L}_{i,j}$  for every  $(i, j) \in E_\sigma$  (Step 2 of the CCA algorithm leaves the non fill-in entries invariant), it follows

that

$$\max_{(i,j) \in E_\sigma} |\hat{L}_{ij} - \bar{L}_{ij}| < \tilde{\delta}$$

on an event  $D_n$  such that  $\bar{P}(D_n) \rightarrow 1$  as  $n \rightarrow \infty$ . Note by Assumption 1 and (S.21) that on  $D_n$

$$\hat{L}_{jj} \geq \bar{L}_{jj} - |\hat{L}_{jj} - \bar{L}_{jj}| \geq \delta - \tilde{\delta} > \frac{\delta}{2}$$

for  $1 \leq j \leq p$ , and

$$|\hat{L}_{ij}| \leq |\bar{L}_{ij}| + |\hat{L}_{ij} - \bar{L}_{ij}| \leq \frac{1}{\delta} + \tilde{\delta} < \frac{2}{\delta}$$

for every  $(i, j) \in E_\sigma$ . It follows that on  $D_n \cap \tilde{D}_n$

$$\begin{aligned} \left| \frac{\hat{L}_{j,j-2}}{\hat{L}_{jj}} - \frac{\bar{L}_{j,j-2}}{\bar{L}_{jj}} \right| &\leq \left| \frac{\hat{L}_{j,j-2}}{\hat{L}_{jj}} - \frac{\hat{L}_{j,j-2}}{\bar{L}_{jj}} \right| + \left| \frac{\hat{L}_{j,j-2}}{\bar{L}_{jj}} - \frac{\bar{L}_{j,j-2}}{\bar{L}_{jj}} \right| \\ &\leq \frac{\hat{L}_{j,j-2}}{\hat{L}_{jj} \bar{L}_{jj}} \left| \hat{L}_{jj} - \bar{L}_{jj} \right| + \frac{|\hat{L}_{j,j-2} - \bar{L}_{j,j-2}|}{\bar{L}_{jj}} \\ &\leq \min \left( \frac{2\tilde{\delta}}{\delta} + \frac{4\tilde{\delta}}{\delta^3}, \left( \frac{2\tilde{K}^*}{\delta} + \frac{4\tilde{K}^*}{\delta^3} \right) \sqrt{\frac{\log p}{n}} \right) \\ &< \min \left( \frac{1-\xi}{2}, \left( \frac{2\tilde{K}^*}{\delta} + \frac{4\tilde{K}^*}{\delta^3} \right) \sqrt{\frac{\log p}{n}} \right), \end{aligned} \quad (\text{S.22})$$

and

$$\left| \frac{\hat{L}_{j,j-2}}{\hat{L}_{jj}} \right| \leq \left| \frac{\bar{L}_{j,j-2}}{\bar{L}_{jj}} \right| + \left| \frac{\hat{L}_{j,j-2}}{\hat{L}_{jj}} - \frac{\bar{L}_{j,j-2}}{\bar{L}_{jj}} \right| < \xi + \frac{1-\xi}{2} = \frac{1+\xi}{2} \quad (\text{S.23})$$

for  $3 \leq j \leq p$ . By similar arguments as above, it can be shown that on  $D_n \cap \tilde{D}_n$

$$\left| \hat{L}_{i,i-2} \frac{\hat{L}_{21}}{\hat{L}_{22}} - \bar{L}_{i,i-2} \frac{\bar{L}_{21}}{\bar{L}_{22}} \right| \leq \frac{8\tilde{K}^*}{\delta^3} \sqrt{\frac{\log p}{n}} \text{ and } \left| \hat{L}_{i,i-2} \frac{\hat{L}_{21}}{\hat{L}_{22}} \right| \leq \frac{8}{\delta^3} \quad (\text{S.24})$$

for  $3 \leq i \leq p$ . Using the identity

$$\left| \prod_{j=1}^k t_j - \prod_{j=1}^k r_j \right| \leq |t_1 - r_1| \prod_{j=2}^k t_j + \sum_{i=2}^{k-1} \left( \prod_{j=1}^{i-1} t_j \right) \left( \prod_{j=i+1}^k r_j \right) |t_i - r_i| + \left( \prod_{j=1}^{k-1} t_j \right) |t_k - r_k|$$

along with (S.19), (S.20), (S.22), (S.23), (S.24) and Assumption  $A3'$ , we obtain

$$|\hat{L}_{i,i-1} - \bar{L}_{i,i-1}| \leq \left( \frac{8\tilde{K}^*}{\delta^3} \left( \frac{1+\xi}{2} \right)^{i-3} + (i-3) \frac{8}{\delta^3} \left( \frac{2\tilde{K}^*}{\delta} + \frac{4\tilde{K}^*}{\delta^3} \right) \left( \frac{1+\xi}{2} \right)^{i-4} \right) \sqrt{\frac{\log p}{n}}$$

for every  $3 \leq i \leq p-1$  on  $D_n \cap \tilde{D}_n$ . Since  $(1+\xi)/2 < 1$ , it follows that for an appropriate constant  $\tilde{K}$

$$\max_{(i,j) \in E_\sigma^D} |\hat{L}_{ij} - \bar{L}_{ij}| \leq \tilde{K} \sqrt{\frac{\log p}{n}}$$

on  $D_n \cap \tilde{D}_n$ . Since  $|E_\sigma| = p$  and  $|E_\sigma^D| = 2p - 3$ , it follows that

$$\|\hat{L} - \bar{L}\|_F^2 \leq \tilde{K} \sqrt{\frac{(|E_\sigma| + 1) \log p}{n}}$$

on  $D_n \cap \tilde{D}_n$ . The bound for  $\|\hat{\Omega} - \bar{\Omega}\|_F$  now follows by similar arguments as those at the end of the proof of Theorem 1.  $\square$

## References

- A. Atay-Kayis and H. Massam. A monte carlo method for computing the marginal likelihood in nondecomposable gaussian graphical models. *Biometrika*, 92:317–335, 2005.
- P. J. Bickel and E. Levina. Covariance regularization by thresholding. *Ann. Statist.*, 36:2577–2604, 2008a.
- P. J. Bickel and E. Levina. Regularized estimation of large covariance matrices. *Ann. Statist.*, 36:199–227, 2008b.
- W.M. Chan and A. George. A linear time implementation of the reverse cuthill-mckee algorithm. *BIT Numerical Mathematics*, 20:1–8, 1980.
- T.A. Davis. *Direct methods for sparse linear systems*. SIAM, Philadelphia, 2006.
- A. P. Dawid and S. L. Lauritzen. Hyper markov laws in the statistical analysis of decomposable graphical models. *Ann. Statist.*, 36:1272–1317, 1993.
- M. Feingold and M. Drton. Robust graphical modeling of gene networks using classical and alternative t-distributions. *Annals of Applied Statistics*, 5:1057–1080, 2011.
- R. Grone, C. Johnson, E. Sá, and H. Wolkowicz. Positive definite completions of partial hermitian matrices. *Linear Algebra and its Applications*, 58:109–124, 1984. ISSN 0024-3795. doi: [https://doi.org/10.1016/0024-3795\(84\)90207-6](https://doi.org/10.1016/0024-3795(84)90207-6). URL <https://www.sciencedirect.com/science/article/pii/0024379584902076>.
- D. Guillot, B. Rajaratnam, and J. Emile-Geay. Statistical paleoclimate reconstructions via markov random fields. *Annals of Applied Statistics*, 9:324–352, 2015.
- H. Hara and A. Takemura. A localization approach to improve iterative proportional scaling in gaussian graphical models. *Communications in Statistics - Theory and Methods*, 39(8-9):1643–1654, 2010. doi: [10.1080/03610920802238662](https://doi.org/10.1080/03610920802238662). URL <https://doi.org/10.1080/03610920802238662>.
- D. A. Harville. Maximum likelihood approaches to variance component estimation and to related concepts. *Journal of the American Statistical Association*, 72:320–338, 1977.
- T. Hastie, R. Tibshirani, and J. Friedman. *Elements of Statistical Learning*. Springer-Verlag, 2009.
- A. Hero and B. Rajaratnam. Hub discovery in partial correlation graphs. *IEEE Transactions on Information Theory*, 58:6064–6078, 2012.

- S. Hojsgaard and S. L. Lauritzen. On some algorithms for estimation in gaussian graphical models. *arXiv*, 2023.
- C. Hsieh, M. Sustik, I. Dhillon, P. Ravikumar, and R. Poldrack. Big & quic: Sparse inverse covariance estimation for a million variables. *Advances in neural information processing systems*, 26, 2013.
- J. Huang, N. Liu, M. Pourahmadi, and L. Liu. Covariance selection and estimation via penalised normal likelihood. *Biometrika*, 93:85–98, 2006.
- K. Khare and B. Rajaratnam. Sparse matrix decompositions and graph characterizations. *Linear Algebra and its Applications*, 437(3):932–947, 2012. ISSN 0024-3795. doi: <https://doi.org/10.1016/j.laa.2012.03.027>. URL <https://www.sciencedirect.com/science/article/pii/S0024379512002583>.
- K. Khare, S. Oh, and B. Rajaratnam. A convex pseudo-likelihood framework for high dimensional partial correlation estimation with convergence guarantees. *Journal of the Royal Statistical Society B*, 77:803–825, 2015.
- K. Khare, B. Rajaratnam, and A. Saha. Bayesian inference for gaussian graphical models beyond decomposable graphs. *Journal of the Royal Statistical Society. Series B (Statistical Methodology)*, 80(4):pp. 727–747, 2018. ISSN 13697412, 14679868. URL <https://www.jstor.org/stable/26773177>.
- Kshitij Khare, Sang-Yun Oh, Syed Rahman, and Bala Rajaratnam. A scalable sparse cholesky based approach for learning high-dimensional covariance matrices in ordered data. *Machine Learning*, 108(12):2061–2086, 2019. doi: 10.1007/s10994-019-05810-5. URL <https://doi.org/10.1007/s10994-019-05810-5>.
- S.L. Lauritzen. *Graphical models*. Oxford University Press Inc., 1996.
- O. Ledoit and M. Wolf. Improved estimation of the covariance matrix of stock returns with an application to portfolio selection. *Journal of Empirical Finance*, 10:603–621, 2003.
- A. Lenkoski. A direct sampler for G-Wishart variates. *Stat*, 2:119–128, 2013.
- G. Letac and H. Massam. Wishart distributions for decomposable graphs. *The Annals of Statistics*, 35(3):1278 – 1323, 2007. doi: 10.1214/009053606000001235. URL <https://doi.org/10.1214/009053606000001235>.
- B. Marjanovic. Huge stock market dataset, 2017. <https://www.kaggle.com/datasets/borismarjanovic/price-volume-data-for-all-us-stocks-etfs>.
- N. Mitsakakis, H. Massam, and M. D. Escobar. A Metropolis-Hastings based method for sampling from the G-Wishart distribution in Gaussian graphical models. *Electron. J. Statist.*, 5:18–30, 2011.
- V.I. Paulsen, S.C. Power, and A.A. Smith. Schur products and matrix completions. *Journal of Functional Analysis*, 85:151–178, 1989.
- J. Peng, P. Wang, N. Zhou, and J. Zhu. Partial correlation estimation by joint sparse regression models. *Journal of the American Statistical Association*, 104:735–746, 2009.

- B. Rajaratnam, H. Massam, and C.M. Carvalho. Flexible covariance estimation in graphical gaussian models. *Ann. Statist.*, 36:2818–2849, 2008.
- A. Rothman, P. Bickel, E. Levina, and J. Zhu. Sparse permutation invariant covariance estimation. *Electronic Journal of Statistics*, 2(none):494 – 515, 2008. doi: 10.1214/08-EJS176. URL <https://doi.org/10.1214/08-EJS176>.
- A. Rothman, E. Levina, and J. Zhu. Generalized thresholding of large covariance matrices. *Journal of the American Statistical Association*, 104(485):177–186, 2009.
- A. Roverato. Hyper inverse wishart distribution for non-decomposable graphs and its application to bayesian inference for gaussian graphical models. *Scandinavian Journal of Statistics*, 29:391–411, 2002.
- A. Shojaie and G. Michailidis. Penalized likelihood methods for estimation of sparse high-dimensional directed acyclic graphs. *Biometrika*, 97:519–538, 2010.
- T.P. Speed and H.T. Kiveri. Gaussian markov distributions over finite graphs. *Annals of Statistics*, 14:138–150, 1986.
- R. Vershynin. *Introduction to the non-asymptotic analysis of random matrices*, Chapter 5 of *Compressed Sensing: Theory and Applications*, edited by Eldar, Yonina C. and Kutyniok, Gitta. Cambridge University Press, 2012. doi: 10.1017/CBO9780511794308.006.
- R. Xiang, K. Khare, and M. Ghosh. High dimensional posterior convergence rates for decomposable graphical models. *Electron. J. Statist.*, 9:2828–2854, 2015.
- P. Xu, J. Guo, and X. He. An improved iterative proportional scaling procedure for gaussian graphical models. *Journal of Computational and Graphical Statistics*, 20(2):417–431, 2011. doi: 10.1198/jcgs.2010.09044. URL <https://doi.org/10.1198/jcgs.2010.09044>.
- P. Xu, J. Guo, and M. Tang. An improved hara-takamura procedure by sharing computations on junction tree in gaussian graphical models. *Statistics and Computing*, 22(5):1125–1133, 2012. doi: 10.1007/s11222-011-9286-4. URL <https://doi.org/10.1007/s11222-011-9286-4>.
- P. Xu, J. Guo, and M. Tang. A localized implementation of the iterative proportional scaling procedure for gaussian graphical models. *Journal of Computational and Graphical Statistics*, 24(1):205–229, 2015. doi: 10.1080/10618600.2014.900499. URL <https://doi.org/10.1080/10618600.2014.900499>.
- G. Yu and J. Bien. Learning local dependence in ordered data. *Journal of Machine Learning Research*, 18:1–60, 2017.
- J. Zhang, M. Wang, Q. Li, S. Wang, X. Chang, and B. Wang. Quadratic sparse gaussian graphical model estimation method for massive variables. In *Proceedings of the Twenty-Ninth International Conference on International Joint Conferences on Artificial Intelligence*, pages 2964–2972, 2021.